Earth Syst. Sci. Data Discuss., doi:10.5194/essd-2017-6, 2017
Manuscript under review for journal Earth Syst. Sci. Data
Discussion started: 20 February 2017

Open Access Earth System Science Data Discussions

Continuous records of the atmospheric greenhouse gases CO_2, CH_4, and N_2O and their radiative forcing since the penultimate glacial maximum

Peter Köhler[1], Christoph Nehrbass-Ahles[2], Jochen Schmitt[2], Thomas F. Stocker[2], and Hubertus Fischer[2]

[1]Alfred-Wegener-Institut Helmholtz-Zentrum für Polar-und Meeresforschung (AWI), P.O. Box 12 01 61, 27515 Bremerhaven, Germany

[2]Climate and Environmental Physics, Physics Institute, and Oeschger Centre for Climate Change Research, University of Bern, Bern, Switzerland

Correspondence to: Peter Köhler (Peter.Koehler@awi.de)

Abstract. Continuous records of the atmospheric greenhouse gases (GHGs) CO_2, CH_4, and N_2O are necessary input data for transient climate simulations and their related radiative forcing important components in analyses of climate sensitivity and feedbacks. Since the available data from ice cores are discontinuous and partly ambiguous a well-documented decision process during data compilation followed by some interpolating post-processing are necessary to obtain those desired time series. Here we document our best-guess data compilation of published ice core records and recent measurements on firn air and atmospheric samples covering the time window from the penultimate glacial maximum (∼156 kyr BP) to the beginning of year 2016 CE. A smoothing spline method is applied to translate the discrete and irregularly spaced data points into continuous time series. These splines are assumed to represent the evolution of the atmospheric mixing ratios for the three GHGs. Global-mean radiative forcing for each GHG is computed using well-established, simple formulations. Newest published age scales are used for the ice core data. While CO_2 is representing an integrated global signal, we compile only a southern hemisphere record of CH_4 and identify how much larger a northern hemisphere or global CH_4 record might have been due to its interhemispheric gradient. Data resolution and uncertainties are considered in the spline procedure and typical cutoff periods, defining the degree of smoothing, range from 5000 years for the less resolved older parts of the records to 4 years for the densely-sampled recent years. The data sets describe seamlessly the GHG evolution on orbital and millennial time scales for glacial and glacial-interglacial variations and on centennial and decadal time scales for anthropogenic times. Data connected with this paper, including raw data and final splines, are available at https://doi.pangaea.de/10.1594/PANGAEA.871273.

1 Introduction

Our knowledge of changes in the atmospheric mixing ratios of the important greenhouse gases (GHGs) CO_2, CH_4 and N_2O beyond the instrumental record is mainly based on discrete data points derived from gas extractions in polar ice cores. While there are recent developments towards continuous CH_4 records using gas extraction and measurement systems coupled to continuous flow analysis systems (Schüpbach et al., 2009; Chappellaz et al., 2013; Rhodes et al., 2013, 2015), none of this is within sight for CO_2 and N_2O, the other two important GHGs, whose changes influence global climate via their radiative forcing. To

Earth Syst. Sci. Data Discuss., doi:10.5194/essd-2017-6, 2017
Manuscript under review for journal Earth Syst. Sci. Data
Discussion started: 20 February 2017

obtain continuous GHG records, which are necessary to force transient climate simulations, these discrete data therefore have to be processed in order to extract those variabilities which have a climatological meaning and to account for measurement uncertainties.

All three GHG records have special features which need some attention during data compilation:

- For some of the CO_2 records obtained from different ice cores apparent, still unexplained offsets exist, e.g. Ahn et al. (2012); Bereiter et al. (2012); Marcott et al. (2014); Bauska et al. (2015). These offsets need to be addressed in our data compilation.

- Due to the dominance of CH_4 sources in the northern hemisphere the CH_4 concentrations are higher in records from Greenland than from Antarctica (referred to as interpolar difference, e.g. Baumgartner et al., 2012).

- *In situ* production of N_2O connected to high mineral dust values led to unreliable values in N_2O (e.g. Schilt et al., 2010a), implying that for glacial peak times and records from Greenland special care has to be taken during data selection.

Rapid changes are most pronounced in CH_4 and N_2O (and to some extend in also in CO_2) during millennial-scale climate variability, or the so-called Dansgaard/Oeschger (D/O) events. Only well synchronised ice cores from Greenland and Antarctica can therefore be used when records from the northern and the southern hemisphere are to be merged into one global record. However, even with the recent efforts on ice core age scale development this north-south synchronisation is not yet perfect in AICC2012 (Veres et al., 2013), the Antarctic Ice Core Chronology of four major Antarctic ice cores. For example, in a recent paper (Baumgartner et al., 2014) inconsistencies in the timing of CH_4 in the ice cores NGRIP, EDML and Talos Dome (TALDICE) have been identified for several D/O event transitions. Furthermore, when comparing data from the West Antarctic Ice Sheet Divide ice core (WDC) on its most recent age scale WD2014 with data from Greenlandic ice cores, the chronology of the latter (GICC05) has been stretched by 0.63% in order to find the best match to the absolute U/Th-dated paleo record of Hulu Cave (WAIS Divide Project Members, 2015).

All these issues need to be addressed and ask for well-motivated data selection and processing. Here we will provide a documentation of our motivations during data compilation and will calculate from those selected GHG data continuous time series of CO_2, CH_4, and N_2O via spline-smoothing (Enting, 1987; Bruno and Joos, 1997) with a nominal temporal resolution Δt of 1 year from the penultimate glacial maximum until present, the time window of interest for PALMOD, the German Paleo Modelling Project (www.palmod.de). Note, however, that this Δt represents not the true resolution but only the typical spline average for each year and that the ice core information represents a low-pass filtered signal of atmospheric variability concentrations by the slow bubble enclosure process to start with. Furthermore, the resulting spline is of restricted use for in-depth analysis with focus on the rates of changes in the three GHGs, since the spline smoothing surpresses the most abrupt changes in the GHGs. The ice core-based paleo records will be extended by instrumental data until the beginning of year 2016 CE including several decades of overlap of ice core and instrumental data. The resulting continuous GHG records might also be of interest and used in the Last Deglaciation experiment within PMIP4 (Ivanovic et al., 2016).

Earth Syst. Sci. Data Discuss., doi:10.5194/essd-2017-6, 2017
Manuscript under review for journal Earth Syst. Sci. Data
Discussion started: 20 February 2017

Open Access Earth System Science Data Discussions

Previous splines (similar to our approach here, but in detail not identical) have also been proposed to be used in interglacial experiments of the Holocene within PMIP4 (Otto-Bliesner et al., 2016). Within the most recent model intercomparison project, CMIP6, a slightly different compilation of GHGs for historical times or the Common Era has been presented (Meinshausen et al., 2016). While this alternative approach has its focus on the time since 1850 CE, its data compilation nevertheless extends back until the year 0 CE, based beyond instrumental times solely on the Law Dome ice core (MacFarling-Meure et al., 2006; Rubino et al., 2013). We will finally compare our splines with these forcing data sets proposed by Meinshausen et al. (2016) to be used within CMIP6.

As will be seen in detail in the next section the mathematical formulation of the spline smoothing method needs as input data some information on the uncertainties or errors of the data points supporting the spline. These data uncertainties taken here are the precisions of individual measurements (1σ errors) and are of the order of a few ppm for CO_2 or a few ppb for CH_4 or N_2O. The uncertainty in the final spline, however, is larger, since the applied smoothing, which depends on the chosen cutoff periods, adds some additional uncertainty. Furthermore, the estimates of the radiative forcing based on these three GHGs are even more uncertain, since the calculations of the radiative forcing themselves are based on models (Myhre et al., 1998) with an embedded intrinsic uncertainty of about $\sim 10\%$.

Please note, that in the following we choose to state that the anthropogenic activities (or emissions) started at 1750 CE (or 200 BP). This is approximately the time, at which both CO_2 and CH_4 in our final splines started to rise rapidly. We keep to this distinction of anthropogenic and pre-anthropogenic changes in the GHGs at 1750 CE throughout the text, although the onset of the Anthropocene is still debated (e.g. Lewis and Maslin, 2015; Steffen et al., 2016; Williams et al., 2016).

2 Details on the spline smoothing method

The numerical code for spline smoothing is based on Enting (1987), but see also Bruno and Joos (1997); Enting et al. (2006) for further details, discussions and applications. It offers the possibility to select different cutoff periods for different time intervals/parts of the input data set, which is needed when data spacing is very different in different parts of the data set.

In a smoothing spline a cost function is minimised. This cost functions includes two terms: (i) the error-weighted deviation between the spline value and the actual data value, and (ii) the curvature of the spline/second derivative. A parameter λ defines how much weight is given to the curvature. The optimisation results in low curvature, i.e. a very smooth spline and relatively large deviations from the original data, for large values of λ. Similarly, increasing errors of the data results in a smoother spline for a given λ. In other words, the smooting of the spline depends on both the assumed errors of the data and the parameter λ.

According to Fourier, each data set can be represented by a sum of sine functions. Ideally, a smoothing spline removes all high frequencies sine functions and acts as a low pass filter. The period (or frequency) where half of the amplitude is attenuated is typically called cutoff period P_{cutoff} (frequency). Thus, periods shorter (frequencies longer) than the cutoff are dampened in the spline. The parameter λ is linked to this cutoff period as described in detail below.

Let us assume input data is t_j, y_j, and v_j corresponding e.g. to time, value, and error (1σ). For a given part of the input data an average error, v, and an average data spacing, Δt, can be computed. The link between the cutoff period (P_{cutoff}), the data

Earth Syst. Sci. Data Discuss., doi:10.5194/essd-2017-6, 2017
Manuscript under review for journal Earth Syst. Sci. Data
Discussion started: 20 February 2017

spacing (Δt), the 1σ error of the input data (v) is:

$$P_{\mathrm{cutoff}} = 2\pi \cdot \left(\lambda \cdot \Delta t \cdot v^2\right)^{0.25} \tag{1}$$

A positive aspect of Eq. 1 is that P_{cutoff} depends only weakly on Δt.

Let us now assume we have a data set where different parts or intervals have very different data spacing and/or for which we would like to apply a different smoothing. We can then modify λ to define an individual P_{cutoff} for each part of the input data set.

Reference interval: λ is computed using Eq. 1 for the given cutoff period, average data spacing, and average error for this first interval. It follows:

$$\lambda = \frac{\left(\frac{P_{\mathrm{cutoff}}}{2\pi}\right)^4}{(\Delta t \cdot v^2)} \tag{2}$$

In the following, the reference interval is always the most recent time window (starting with the beginning of year 2016 CE) covered with instrumental measurements.

Other intervals: A modified $\lambda' = \lambda \cdot s^2$ with λ taken from the reference interval is used here, implying that for the reference interval $s = 1$ and $\lambda' = \lambda$. The scaling factor s is chosen to gain the desired P_{cutoff} after

$$P_{\mathrm{cutoff}} = 2\pi \cdot \left(\lambda \cdot s^2 \cdot \Delta t \cdot v^2\right)^{0.25} \tag{3}$$

following that s is prescribed as:

$$s = \frac{\left(\frac{P_{\mathrm{cutoff}}}{2\pi}\right)^2}{\sqrt{(\lambda \cdot \Delta t)} \cdot v} \tag{4}$$

where Δt and v are the mean data spacing and the mean error for the interval under consideration.

3 Greenhouse gas data compilations and final splines

Our GHG data compilations are based on various different data sets from thirteen global distributed locations. An overview of the locations, including latitude/longitude is obtained in Table 1. Please note, that from some of those locations CH_4 data are taken only for comparison, but are not supporting the spline, since only a southern hemisphere spline is constructed. They are furthermore supported for the instrumental period by some global mean data from the NOAA observational network, including RITS Nitrous Oxide data from the NOAA/ESRL halocarbons program and Nitrous Oxide data from the NOAA/ESRL halocarbons in situ program, consisting of various globally distributed measurement sites. Furthermore, at the level of the individual point in the files uploaded to the data base PANGAEA, the entries from MacFarling-Meure et al. (2006) and Rubino et al. (2013) are all labeled as as "Law Dome" data for simplicity, although these two studies show data from the Law Dome deep ice core and from various shallow cores are combined with atmospheric data from Cape Grim, and South Pole. Please refer to the original publications for a precise characterisation of the sample origins.

Earth Syst. Sci. Data Discuss., doi:10.5194/essd-2017-6, 2017
Manuscript under review for journal Earth Syst. Sci. Data
Discussion started: 20 February 2017

3.1 Atmospheric CO_2

There are offsets in measured CO_2 of unidentified causes between records obtained from different ice cores (e.g. Ahn et al., 2012; Bereiter et al., 2012; Marcott et al., 2014; Bauska et al., 2015). These offsets may be related to inter-laboratory differences in the calibration, or potentially due to *in situ* artefact production of CO_2 in the ice archive. For a detailed discussion see Ahn et al. (2012) and the supplement to Bereiter et al. (2012). Moreover, amplitudes of GHG variations may differ from one core to the other due to the site dependent bubble enclosure characteristics, which leads to more or less low-pass filtering. Offsets require the adjustment of individual records to avoid spurious CO_2 changes when linking different records from different laboratory and ice cores. Ice core data are considered here on the best (most recent) age model available, whose details are contained in Table 2. AICC2012 refers to the most recent Antarctic Ice Cores Chronology providing age models for EDC, EDML, Talos Dome, Vostok, alongside the Greenlandic NGRIP record (Bazin et al., 2013; Veres et al., 2013). The CO_2 record from WDC is used here on its more recent age scale WD2014 to have the timing of CO_2 and the other two GHGs consistently on the same chronology. Using WD2014 instead of the original chronology WDC06A-7 leads to a shift of the timing of the deglacial CO_2 rise during Termination I by about 100 years towards younger ages. The related age difference for an update of the WDC chronology to WD2014 is for CO_2 during the last 1.2 kyr only about 10 years.

Our CO_2 data compilation goes back in time until $\sim$156 kyr BP, at which point in time well-resolved CO_2 records stop. The full CO_2 spline covering the whole time window from 2016 CE to 156 kyr BP is plotted in Fig. 1, including the age distance, Δt, of the compilation of data points in sub-panel B. The 11-points-running mean of Δt is around 100 years in the Holocene, between 20 and 50 years during Termination I, and varies between 40 and 200 years between 20 and 70 kyr BP, rising to 500 to 1000 years later-only with a slightly higher resolution of 200 years only across Termination II.

The CO_2 data contributing to this spline are the following (see also Table 2 for details):

1. We start our CO_2 data compilation at present day (end of year 2015 CE $\widehat{=}$ beginning of year 2016 CE, or -66.0 BP). From the NOAA network instrumental monthly CO_2 data are available online (Dlugokencky et al., 2016b). We here choose to take only the data of the original so-called "Keeling-Curve" started by C.D. Keeling at NOAA's Mauna Loa Observatory in 1958 CE, and since 1974 CE independently measured by both Scripps Institution of Oceanography (scrippsco2.ucsd.edu) and NOAA (www.esrl.noaa.gov/gmd/ccgg/trends/) (Fig. 2A). Please note, that there is a small interhemispheric difference in CO_2 with higher values in the north and lower values in the south, e.g. the 10-years averages from 2006 CE to 2015 CE have been 3.5 ppm smaller at South Pole than at Mauna Loa, and 1.4 ppm higher at Barrow (Alaska) than at Mauna Loa (Dlugokencky et al., 2016b). Hence, CO_2 data from Mauna Loa are only a (very good) approximation to a global value which might be used for calculating radiative forcing. However, in practise this interhemispheric difference does not matter, since no information on it exists beyond the instrumental period: CO_2 is only measured on ice cores from Antarctica, as the higher dust content can give rise to artefacts in any CO_2 measurement based on Greenlandic ice cores (e.g. Anklin et al., 1995; Stauffer et al., 1998).

Earth Syst. Sci. Data Discuss., doi:10.5194/essd-2017-6, 2017
Manuscript under review for journal Earth Syst. Sci. Data
Discussion started: 20 February 2017

Open Access Earth System Science Data Discussions

2. The firn and ice data compilation of Law Dome, which also contains some contributions from Cape Grim and South Pole — available for the time from 1996 CE to 1 CE (-46 BP to 1949 BP) (MacFarling-Meure et al., 2006) and 2001 CE to 154 CE (-51 BP to 1796 BP) (Rubino et al., 2013) — overlap consistently with these direct atmospheric measurements. We therefore take these data as our reference (Fig. 2B), but include only the data from year 1960 CE and older in our spline compilation. In doing so, we use the more precise and temporally higher resolved instrumental data for later times.

3. Data from the WDC ice core exist for the times of 11–1210 BP, or 740–1939 CE (Ahn et al., 2012; Bauska et al., 2015) and for Termination I (see #5 below). These WDC data are overlapping with the Law Dome data (MacFarling-Meure et al., 2006; Rubino et al., 2013). However, as already shown in Ahn et al. (2012) the available high resolution CO_2 records of different ice cores (Law Dome, WDC, EDML) show some apparent offsets. While during the anthropogenic rise in CO_2 after 1750 CE the CO_2 data in all three ice cores converge to similar values, the WDC record seems to show slightly higher values than the other two ice cores prior to that point in time. EDC data not contained in the comparison of Ahn et al. (2012) also agree in the pre-anthropogenic time more with the Law Dome data than with those of WDC. We therefore choose to take WDC data only before the anthropogenic rise (200–1210 BP or 740–1750 CE) and adjust the WDC data by reducing the reported values by 3.13 ppm, which is the mean difference between the WDC and the Law Dome CO_2 records for this interval. Thus, the data from Law Dome and the adjusted data from WDC both contribute to our data compilation during 200–1210 BP. The mean temporal resolution of both ice core CO_2 records within this time interval are 8 and 13 years for WDC and Law Dome, respectively. The amplitude of the CO_2 minima around 300–400 BP is still controversially discussed (Bauska et al., 2015). In our final spline little of the large negative anomaly in CO_2 contained in the Law Dome data is preserved, since we smoothed the ice data in this time window with a cutoff period of 160 years (Fig. 2B). The time after 1750 CE containing the anthropogenic rise and before the start of the instrumental measurements in 1958 CE is in our compilation only supported by the Law Dome data (Fig. 2B). Further details on this adjustment of the WDC data are covered in Figure A1.

4. EDC data exist between 350 BP and the LGM (Monnin et al., 2001, 2004) and further back in time (see #7 below). They overlap with the Law Dome data between 350–1950 BP (Fig. 2B) and therefore no offset correction is applied for the EDC data. However, EDC data are only considered here for the times 1.9–11 kyr BP, because for the more recent times Law Dome and WDC data provide a better resolution, while for the older times across Termination I the WDC data are the higher resolved reference record (Fig. 2C).

5. Termination I is best covered by data from WDC (Marcott et al., 2014). WDC data are available for 22.9–8.8 kyr BP and are adjusted by –6.06 ppm (Fig. 2C). This difference corresponds to the duration-weighted mean offset between the WDC and EDC records during three intervals of relatively constant CO_2 (22.3–18.5 kyr BP: WDC ($n = 29$) 194.75 ± 2.44 ppm; EDC ($n = 21$) 188.22 ± 2.32 ppm; 14.5–13.0 kyr BP: WDC ($n = 45$) 243.02 ± 2.44 ppm; EDC ($n = 9$) 237.57 ± 1.42 ppm; 11.5–9.0 kyr BP: WDC ($n = 36$) 269.97 ± 3.67 ppm; EDC ($n = 27$) 264.24 ± 1.88 ppm). The intervals have been selected to minimise the influence of potential age scale differences between the two records and only those EDC studies focusing on CO_2 measurements (Monnin et al., 2001, 2004) have been considered here, but not those with

Earth Syst. Sci. Data Discuss., doi:10.5194/essd-2017-6, 2017
Manuscript under review for journal Earth Syst. Sci. Data
Discussion started: 20 February 2017

Open Access Earth System Science Data Discussions

main focus on δ^{13}C (Lourantou et al., 2010b; Schmitt et al., 2012), which have a somewhat lower precision in CO_2 concentrations. More details on this adjustment of the WDC data during Termination I are found in Figure A2. These offset corrections imply that the absolute CO_2 concentration is uncertain by about 5 ppm (accuracy). The corresponding radiative forcing following

$$\Delta R_{[\mathrm{CO_2}]} = 5.35 \cdot ln(\mathrm{CO_2}/(278\ \mathrm{ppm}))\ \mathrm{W\ m^{-2}} \tag{5}$$

(Myhre et al., 1998) is 0.15 or 0.09 W m^{-2} for a reference concentration of 180 or 280 ppm, respectively. This is larger than the relative uncertainty (precision) of the order of 1 ppm attached to individual data points which is used to determine the smoothing spline through the data.

6. Further back in time all ice core records attached below have some data overlap with the previous record. There are some small offsets between these different records (for details see Bereiter et al., 2012). We treat them all alike so the spline averages over all cores and choose to select a rather larger cutoff period of 2000 years for the time between LGM and the end of the previous interglacial to account for those uncertainties. Rapid variations in CO_2 in glacial times (Fig. 2D-F) are best covered in the Siple Dome record between 21.9 and 48.7 kyr BP (Ahn and Brook, 2014), the Talos Dome record between 34.4–69.7 kyr BP (Bereiter et al., 2012), and the EDML record between 43.2–113.4 kyr BP (Lüthi et al., 2010; Bereiter et al., 2012). Talos Dome CO_2 data include some outliers which disagree with CO_2 records from other ice cores by more than 10 ppm. Therefore, Talos Dome data are only considered for the times older than 38.0 kyr BP.

7. From 104.3–156.3 kyr BP — covering the last glacial inception, the last interglacial, as well as Termination II and the penultimate glacial maximum (Fig. 2F) — CO_2 is best covered by data from EDC (Schneider et al., 2013; Lourantou et al., 2010a).

For every supporting data point j a 1σ uncertainty or error v_j has to be assigned in order to be able to calculate the smoothing spline (see section 2 for details). Therefore, a nominal uncertainty of 0.3 ppm is assigned to the Mauna Loa data, following information given on the NOAA website. Uncertainties for the ice and firn data are taken either as reported or set to a minimal value of 0.5 ppm if the reported standard deviation is missing or less than 0.5 ppm. For Law Dome data published in MacFarling-Meure et al. (2006) we take a uniform uncertainty of 1.1 ppm as reported in their methods section.

The data selection as described above then leads to $n = 2152$ data points including 20 ages with duplicate entries. These duplicates are removed (reducing n to 2132) and their CO_2 values are calculated from the average of the single values with the assigned uncertainties based on this averaging.

To account for the given age spacing Δt or data frequency of the data points (Fig. 1B) and the knowledge of abrupt changes in CO_2 during Termination I, the spline is divided into 12 intervals with different nominal cutoff periods, which varied between 4 years for instrumental times and 3000 years during most of the Holocene. A low P_{cutoff} of 600 years could be assigned to the now well-covered interval of Termination I (11–18.5 kyr BP). For the glacial times older than 18.5 kyr BP P_{cutoff} of 2000 years has been selected, whose usage is extended until 110 kyr BP. For the warm interglacial between 110 and 128 kyr BP we assign the same cutoff period of 3000 years as has been chosen before for the recent interglacial, the Holocene. Thereafter, we

Earth Syst. Sci. Data Discuss., doi:10.5194/essd-2017-6, 2017
Manuscript under review for journal Earth Syst. Sci. Data
Discussion started: 20 February 2017

Open Access Earth System Science Data Discussions

continue with a 1000 years cutoff period for the CO_2 rise during Termination II (128–135 kyr BP), before again 2000 years are chosen during the penultimate glacial maximum. A summary of all details on the calculated spline is found in Table 3.

The final CO_2 record of the last 2 kyr to be used within CMIP6 (Meinshausen et al., 2016) is (i) within instrumental times nearly indistinguishable from our spline (Fig. 2A) and (ii) in the pre-anthropogenic time of the last 2 kyr partly larger by a few ppm than our spline (Fig. 2B). This difference is readily explained by the underlying data and the different filtering. While we here use a mixture of Law Dome and WDC data between 200 and 1210 BP, only Law Dome data are considered for CMIP6.

The CO_2 values chosen as boundary conditions for several time slice experiments within PMIP4 (Ivanovic et al., 2016; Otto-Bliesner et al., 2016) can be compared with snapshots from our splines (Table 4). However, one needs to be aware that some short-term fluctuations in our spline might offset the values from long-term averages and lead to differences between our final splines and the PMIP4 forcing data. For the Mid-Holocene (6 kyr experiment) both our approach and that of PMIP4 are based on the same EDC data and processed with the identical spline routines and cutoff frequencies, leading to identical values. Values differ by a few ppm for the experiments 1850 CE, 21 kyr and 127 kyr.

Since spline smoothing is a low-pass filter, abrupt changes in CO_2 are always smaller in the spline than in the original data sets. Therefore, if one wants to investigate in great detail the impact of very fast and abrupt rises in CO_2 on the climate system that have been identified during three points in time (around 11.6, 14.7 or 16.2 kyr BP) across Termination I (Monnin et al., 2001; Marcott et al., 2014) an alternative continuous CO_2 record needs to be constructed. One approach might be to further reduce the cutoff period to lower values so that the spline would include these pronounced jumps. In detail, one might want to obtain a rise in CO_2 of 12 and 13 ppm during one century at 16.2 kyr BP and 11.6 kyr BP, respectively, as identified in the WDC record (Marcott et al., 2014). For the abrupt rise in CO_2 around 14.7 kyr BP even an artificial rise of 15 ppm in 200 years, slightly larger than the 12 ppm of the WDC record, has been suggested to represent atmospheric changes in CO_2 potentially caused by permafrost thawing during the northern hemispheric warming into the Bølling/Allerød (Köhler et al., 2014, 2015). Transient simulations forced by records containing these abrupt jumps in CO_2 might be able to investigate their impact in greater detail than simulations forced with our low-frequency spline.

3.2 Atmospheric CH_4

Our data compilation of CH_4 data and the consistently calculated CH_4 spline is restricted to the southern hemisphere (SH). Northern hemispheric (NH) data are shown for comparison, but are not included in the spline, since for such efforts chronologies of ice cores from both hemispheres have to match perfectly during abrupt climate changes of the D/O events. However, as has been shown (Baumgartner et al., 2014) this is not the case for the most recent chronology AICC2012. NH CH_4 and consequently global CH_4 values should according to the well-known interhemispheric gradient be larger than our SH CH_4 values. Therefore, our SH CH_4 spline consists of a lower bound of CH_4 values. Baumgartner et al. (2012) found that NH CH_4 was up to +4% (+14 ppb) and +10% (+60 ppb) larger than in the SH during glacial times and the Holocene, respectively. Using an approximation of the radiative forcing

$$\Delta R_{[CH_4]} \sim 1.4 \cdot 0.036 \cdot (\sqrt{CH_4/\text{ppb}} - \sqrt{742})\ \text{W m}^{-2}, \tag{6}$$

Earth Syst. Sci. Data Discuss., doi:10.5194/essd-2017-6, 2017
Manuscript under review for journal Earth Syst. Sci. Data
Discussion started: 20 February 2017

which neglects the interacting effects of CH_4 and N_2O (Myhre et al., 1998), but which considers the approximately increase in $\Delta R_{[CH_4]}$ by 40% through indirect effects of CH_4 on stratospheric H_2O and tropospheric O_3 (Hansen et al., 2005; Köhler et al., 2010), we estimate that this restriction of CH_4 to the SH only might underestimate the radiative forcing of CH_4 by less than 0.05 W m^{-2}.

Our data compilation starts, identical to that for CO_2, (end of year 2015 CE $\widehat{=}$ beginning of year 2016 CE; -66.0 BP) and stops around 156 kyr BP, to cover the same time window as for CO_2 (Fig. 3A). The 11-points-running mean age distance between neighbouring data points, Δt, is less than 100 year for most of the last 60 kyr, increasing to ~700 years further back in time (Fig. 3B). Our strategy here is to select one (best) data set for each point in time, and use overlapping intervals only for confirmation of data consistency and the absence of any offsets in CH_4. In detail, the following data sets are considered here:

1. From the NOAA network annual global mean values of CH_4 from 2016 CE back to 1984 CE are available (www.esrl.noaa.gov/gmd/ccgg/trends/). They are clearly positioned between the seasonally resolved data from Barrow, Alaska (NH), and South Pole (SH), both reaching back in time until 1983 CE (Dlugokencky et al., 2016a) (Fig. 4A). The interhemispheric gradient of the NH (Barrow) to the SH (South Pole) was at the beginning of 2016 CE with +161 ppb or +9% larger than in the Holocene. An estimation of the radiative forcing of this interhemispheric gradient reveals that for this most recent time the $\Delta R_{[CH_4]}$ for the NH was by less than 0.1 W m^{-2} larger than for the SH. For our SH compilation we used the South Pole data.

2. Ice core and firn air data from Law Dome and Cape Grim (SH) exist from 2005 CE back to 14 CE (= 1936 BP) (MacFarling-Meure et al., 2006; Rubino et al., 2013) with an overlap of more than two decades with the instrumental measurements (Fig. 4A,B). The CH_4 data from this record, which are taken in support of the spline, are nevertheless restricted to the two centuries between 1982 CE and 1782 CE (= 168 BP) bridging the gap between instrumental data and CH_4 from WDC. Where the Law Dome data overlap with the data from either South Pole or WDC no apparent offset between the different data sets has be identified.

3. The discrete CH_4 data from WDC (SH) start at 169 BP, going back in time to 67 kyr BP (WAIS Divide Project Members, 2015; Marcott et al., 2014; Buizert et al., 2015; Mitchell et al., 2013, 2011; Sigl et al., 2016). Right now WDC CH_4 are the highest resolved data of the last glacial times and therefore our reference record (Fig. 4B-E). The data do not only contain the well known abrupt CH_4 changes at the onset and end of the millennial-scale D/O events in high resolution and accuracy, but also centennial-scale features, which are also understood to be of climatic origin (e.g. Mitchell et al., 2013).

4. We continue our SH CH_4 data compilation at the end of what is covered in WDC with data from EDC, covering 67 kyr BP – 156 kyr BP (Loulergue et al., 2008) (Fig. 4E-F). These EDC data would in principle go back in time over the whole 800 kyr covered by the EDC ice core, but since our focus here is on approximately the time since the penultimate glacial maximum (or approximately the last 156 kyr), those data further back in time are not taken into consideration.

5. The NH Greenland composite of CH_4 (Blunier and Brook, 2001; Dällenbach et al., 2000; Flückiger et al., 2004; Landais et al., 2004) is only plotted for comparison to the SH data (Fig. 4B-F).

Assigned data uncertainty (1σ error) is 2.0, 4.0, 2.4, and 10 ppb for instrumental data, Law Dome, WDC, and EDC, respectively, based on published information (Dlugokencky et al., 2016a; MacFarling-Meure et al., 2006; Mitchell et al., 2013; Loulergue et al., 2008). Using the approximation of $\Delta R_{[CH_4]}$ given above these 1σ error are related to uncertainties in the radiative forcing of less than 0.01 W m^{-2}.

Compiled data contain 2990 data points, from which for 37 ages duplicate entries exits. These duplicates are removed giving $n = 2953$ and for those ages new values (mean, uncertainties) are calculated.

The whole data set is divided in nine intervals with different assigned cutoff periods. P_{cutoff} ranges from 4 years for the interval covered by instrumental data to 60 years during Termination I and the LGM. Due to lower data coverage further back in time P_{cutoff} is then increased to 200 (23–60 kyr BP), 500 (60–128 kyr BP), and 1000 years (128–156 kyr BP). More details are shown in Table 6.

The SH CH_4 record to be used within CMIP6 (Meinshausen et al., 2016) largely agrees with our SH spline (Fig. 4A,B). However, during instrumental times the CMIP6 SH CH_4 record is consistently larger than our SH spline by about 10–15 ppb, probably caused by the consideration of various different stations in the calculation of the SH CH_4 record within CMIP6, while we here only rely on South Pole data. Prior to the instrumental CH_4 data around 1980 CE the difference between both approaches is with 30 ppb largest. This might be caused by the statistical routines within CMIP6 to account for missing stations. Further back in time (around 1150 BP, 1300 BP, 1900 BP) higher frequency variation contained in the WDC CH_4 record (used here, but ignored within CMIP6) leads to some CH_4 variabilities on the order 10–25 ppb within our SH spline, that are not contained within the CMIP6 SH CH_4 record.

A comparison of our final spline with the GHG values chosen for the PMIP4 time slice experiments (Ivanovic et al., 2016; Otto-Bliesner et al., 2016) is not straight-forward, since we here only compile SH CH_4 data, while the PMIP4 experiments need and use global values. Taking the two records at face value one finds that our SH CH_4 is 13, 44, 25 ppb smaller than the global mean value used in PMIP4 for 1850 CE, 6 kyr, 127 kyr, respectively. Especially, the large SH-global difference of 44 ppb around 6 kyr seems to be rather large, but is readily explained by the centennial variability contained in the WDC CH_4 which leads to a local minimum in SH CH_4 around 6 ka. Furthermore, our SH CH_4 spline is 7 ppb higher than the global CH_4 value chosen within PMIP4 for the 21 kyr experiment, again explained by the centennial-scale variability contained in the WDC CH_4 record, with a local maximum just at 21 kyr BP. Hundred years later, our SH CH_4 spline has a local minimum which is 11 ppb smaller than the global CH_4 values taken for PMIP4 (Table 4).

3.3 Atmospheric N_2O

For the data compilation of the third GHG, N_2O, one has to be aware that during times of high dust input *in situ* production of N_2O might occur leading to artefacts in the paleo record (Schilt et al., 2010a). Furthermore, the precise synchronisation of northern and southern hemisphere records, as already explained for CH_4, is crucial to get changes in N_2O during millennial-scale D/O events right.

The compiled record, again, starts at the end of year 2015 CE (≙ beginning of year 2016 CE; −66.0 BP), but extends back in time only until ∼134.5 kyr BP (Fig. 5A), because the ice cores on which the N_2O compilation is based on in the older parts, Talos Dome, EDC and NGRIP, have no data points between 134.5 and 156 kyr BP, or only unreliable N_2O data containing artefacts are reported in the pen-ultimate glacial maximum (Schilt et al., 2010a). The latter is also the case for EDML, whose data have not been taken to support the spline, since in large parts N_2O of EDML and EDC agree, and the data from EDML have a lower temporal resolution than those of EDC (Schilt et al., 2010a).

In detail, the data sets contributing to the N_2O stack are the following:

1. There are two contributions of N_2O data based on instrumental measurements to the NOAA network or ESRL halocarbon program: (a) *in situ* data from 2016 CE back until 1999 CE, and (b) the RITS N_2O data from 2000 CE back until 1988 CE, both representing global mean monthly values (Fig. 6A). Note that due to the long atmospheric lifetime of N_2O, any interhemispheric gradient can be safely neglected.

2. Law Dome and Cape Grim N_2O data exist from 2004 CE back until 13 CE (= 1937 BP) (MacFarling-Meure et al., 2006), overlapping nicely with the instrumental data (Fig. 6A,B). Here, the Law Dome data contribute to the spline only for those years not covered by the instrumental record, so from 1983 CE and earlier.

3. In the Holocene N_2O was measured at EDC (Flückiger et al., 2002) from 334 BP until 11.5 kyr BP. For the last two millennia the EDC N_2O data points are sparser than the Law Dome data, therefore the EDC N_2O data are only considered for times older than what is covered in the Law Dome N_2O record, in detail before 1975 BP (Fig. 6B,D).

4. The highest resolved N_2O record for large parts of Termination I are based on the horizontal ice core from Taylor Glacier (Schilt et al., 2014) which has been linked to the chronology of the WDC ice core (WD2014) via CH_4 (Baggenstos, 2015). In detail, the Taylor Glacier N_2O record covers the time window 9.6 to 15.8 kyr BP (Fig. 6C) and is taken to support our spline.

5. The last glacial interval is well covered by data from the NGRIP record from Greenland (Flückiger et al., 2004; Schilt et al., 2010b, 2013). While the data cover the times between 11 kyr BP and 119.6 kyr BP, we only take those data older than 15 kyr BP due to the higher resolved Taylor Glacier N_2O data during Termination I (Fig. 6C-F). Furthermore, five data points near the bedrock in the bottom part of the NGRIP records have apparent higher N_2O values than found in ice cores from the southern hemisphere. These data points are rejected here, leading to the oldest NGRIP N_2O data point at 118.6 kyr BP. We are aware that due to the imperfect north-south synchronization of gas records in AICC2012 (see subsection 3.2 for details) the usage of N_2O data from NGRIP might introduce erroneous phasing between N_2O and the purely SH-based CH_4 spline during abrupt change connected to D/O events. However, N_2O data coverage in the SH core

Earth Syst. Sci. Data Discuss., doi:10.5194/essd-2017-6, 2017
Manuscript under review for journal Earth Syst. Sci. Data
Discussion started: 20 February 2017

Open Access Earth System Science Data Discussions

is very sparse and a spline only based on SH data seems to be even less reliable. This potential synchronization problem is also addressed by large cutoff periods of the spline of 2000 to 5000 years beyond 16 kyr BP.

6. Additional N_2O data going back to 134.4 kyr BP are obtained from the Talos Dome ice core (Schilt et al., 2010b) and from further data of the EDC ice core (compilation found in Schilt et al. (2010a); data source between 29.0–134.5 kyr BP: Stauffer et al. (2002); Spahni et al. (2005)). Since these are — besides EDML which very much agrees with EDC (Schilt et al., 2010a) — the only N_2O records with reliable data going back into the penultimate glacial maximum we consider all data points from these ice cores here before 15 kyr BP. The data points of Talos Dome and EDC in general agree with the NGRIP data over the last glacial cycle, but NGRIP diverges from the SH records towards higher (probably biased) values in the warm previous interglacial around 115 kyr BP. As already explained above, these 5 NGRIP data points are rejected. However, across Termination I Talos Dome N_2O data seems to be systematically lower than NGRIP N_2O data, with Taylor Glacier data in-between both (Fig. 6C). We therefore believe, that a mixture of all three records, N_2O from NGRIP, EDC and Talos Dome, most likely covers a reasonable mean global N_2O value (Fig. 6C-F). The relatively large difference in N_2O from different ice cores during the last glacial times indicates, that the uncertainty (accuracy) in N_2O is probably higher than the reported measurement errors (precision) of about 10 ppb.

The general assigned 1σ uncertainty of each data point is 7 ppb for the Law Dome ice core (MacFarling-Meure et al., 2006). Uncertainty of individual data points in other ice cores was in general less than 7 ppb (Flückiger et al., 2002; Schilt et al., 2014). For 58 times more than one data point for the same age exists. These duplicates are removed and the calculated mean and standard deviation of the averaging procedure (if larger than reported measurement error) are taken, reducing the amount of N_2O data to $n = 2344$. For the instrumental measurements we take the reported uncertainties of around 1 ppb. Using an estimate of the radiative forcing of N_2O, which neglects the interacting effects of CH_4 and N_2O

$$\Delta R_{[\mathrm{N_2O}]} \sim 0.12 \cdot (\sqrt{\mathrm{N_2O/ppb}} - \sqrt{272})\ \mathrm{W\ m^{-2}}, \tag{7}$$

(Myhre et al., 1998), we estimate that the 1σ error in N_2O is related to an uncertainty in the radiative forcing of about 0.04 W m^{-2}, so slightly larger than the uncertainty in ΔR related to the CH_4 data. Comparing the different values of N_2O in Talos Dome and NGRIP for same points in time reveals also differences on other order of about 10 ppb (e.g. Fig. 6C-F), suggesting that the ice core specific values of N_2O contain an intrinsic uncertainty of similar size than the measurement error.

The mean age distance (11-points-running mean) of the underlying N_2O data is around 50 years during large parts of the last glacial cycle (15–60 kyr BP), with slightly lower resolution of 100 years in the Holocene and between 60–115 kyr BP. In MIS5.5, Termination II and the penultimate glacial maximum the mean age distance rises to ~500 years (Fig. 5B). Based on this distribution of Δt the prescribed cutoff periods for the spline varies for 7 different intervals between 4 years for the instrumental times to 5000 years for data older than 117 kyr BP. For a large part of the data (400 yr BP to 117 kyr BP) a P_{cutoff} between 500 and 2000 years is prescribed. More details on the spline are found in Table 8.

If compared with the N_2O compilation used within CMIP6 (Meinshausen et al., 2016) both approaches largely agree for instrumental times (Fig. 6A). Further back in time during the last 2 kyr, both approaches rely on the same data: the published

Earth Syst. Sci. Data Discuss., doi:10.5194/essd-2017-6, 2017
Manuscript under review for journal Earth Syst. Sci. Data
Discussion started: 20 February 2017

Law Dome / Cape Grim N_2O data (MacFarling-Meure et al., 2006). Interestingly both time series differ by up to 6 ppb between 0.7 and 2.0 kyr BP (Fig. 6B). This difference is in the range of the ice core data uncertainty, and therefore still small, but we have no easy explanation at hand. Compared with our data compilation the records used in CMIP6 are higher than all data from Law Dome or other SH ice cores (Fig. 6B), for some apparent unknown reason.

The N_2O data used as starting values in the PMIP4 experiments 1850 CE, 6 kyr, 21 kyr, 127 kyr (Ivanovic et al., 2016; Otto-Bliesner et al., 2016) agree within 1 or 2 ppb with values based on our calculated spline, only for 21 kyr the offset is 6 ppb (Table 4).

4 Conclusions

Based on our best knowledge we have compiled available greenhouse gas records and by calculating a smoothing spline we were able to provide continuous records over the last glacial cycle, starting from the beginning of year 2016 CE and ranging back in time until 134 kyr BP for N_2O and until about 156 kyr BP for CO_2 and CH_4. These records should serve as radiative forcing in transient climate simulations as planned, for example, in the German project PALMOD, or might be used in the Last Deglaciation experiment within PMIP4 (Ivanovic et al., 2016) or in other future MIP.

The resulting radiative forcing of the three GHGs calculated here with the simplifed non-interacting Eqns. 5–7 have relative uncertainties of ∼10% (Myhre et al., 1998). The results are very similar to recent calculations based on a complete and revised set of simplified equations, which consider also interacting effects between the three GHGs (Etminan et al., 2016), with differences between old and new expressions in $\Delta R_{[CO_2]}, \Delta R_{[CH_4]}$, and $\Delta R_{[N_2O]}$ of less than 0.01, 0.04, and 0.02 W m^{-2}, respectively. While the difference in $\Delta R_{[CO_2]}$ and $\Delta R_{[N_2O]}$ lie within their uncertainty bands, that of $\Delta R_{[CH_4]}$ is slightly higher, leading also to a revised relative uncertainty of 14% (Etminan et al., 2016). We nevertheless refrain from applying the new equations throughout the study, since the amplification in $\Delta R_{[CH_4]}$ by 40% through indirect effects of CH_4 (Hansen et al., 2005) is not yet considered therein, and we prefer to estimate the radiative forcing of one of the three GHGs individually without interacting effects. These forcing calculations nicely illustrate the dominant contribution of CO_2, which is responsible for about two thirds of the total radiative forcing $\Delta R_{[GHG]}$ during both the anthropogenic rise (Fig. 7A) and the reduction during the LGM (Fig. 7B). The higher resolved variability in CH_4, resulting from smaller cutoff periods during spline calculations than for CO_2, also imposes some fine-scale structure on the overall GHG radiative forcing (Fig. 7C,D), however, dominant features are still mainly provided by CO_2.

5 Acknowledgements

We thank NOAA for data availability of the instrumental GHG data, in detail Ed Dlugokencky and Pieter Tans, NOAA/ESRL (www.esrl.noaa.gov/gmd/ccgg/trends/) and Ralph Keeling, Scripps Institution of Oceanography (scrippsco2.ucsd.edu/). Furthermore, we thank Fortunat Joos for some earlier thoughts on similar GHG data compilations and for providing the Fortran routines to calculate the spline fits. We thank Rainer Sieger (PANGAEA data base) for comments on the uploaded data, which led to the preparation of Table 1 (summary on data sites). This is a contribution to the German BMBF project PALMOD. Long-term support of ice core research at the University of Bern by the Swiss National Science Foundation (SNF) is gratefully acknowledged.

6 Data Availability

Data connected with this paper are available in the scientific data base PANGAEA (https://doi.pangaea.de/10.1594/PANGAEA.871273).
In detail, for each of three GHGs the following data are available:

- Finally compiled raw data (t_j, y_j, v_j corresponding to time, value, assumed 1σ-error), including the data source, as described in the article.
- Pre-processed raw data (averaging of duplicate entries for similar times)
- Calculated splines with time steps of $\Delta t = 1$ year.
- Corresponding radiative forcing based on the simplified Eqns. 5–7.

When using these data please consider citing the original publications from which the data underlying this compilation have been taken.

7 Author Contribution

PK initiated the work, compiled the data, calculated the spline and led the writing of the manuscript. CNA, JS, TFS, and HF contributed specific insights on the data selection and advised the spline smoothing. All co-authors commented on and improved the initial draft.

References

Ahn, J. and Brook, E. J.: Siple Dome ice reveals two modes of millennial CO_2 change during the last ice age, Nature Communications, 5, 3723, doi:10.1038/ncomms4723, 2014.

Ahn, J., Brook, E. J., Mitchell, L., Rosen, J., McConnell, J. R., Taylor, K., Etheridge, D., and Rubino, M.: Atmospheric CO_2 over the last 1000 years: A high-resolution record from the West Antarctic Ice Sheet (WAIS) Divide ice core, Global Biogeochemical Cycles, 26, GB2027, doi:10.1029/2011GB004247, 2012.

Anklin, M., Barnola, J. M., Schwander, J., Stauffer, B., and Raynaud, D.: Processes affecting the CO_2 concentrations measured in Greenland ice, Tellus B, 47, 461–470, 1995.

Baggenstos, D.: Taylor Glacier as an archive of ancient ice for large-volume samples: Chronology, gases, dust, and climate, Ph.D. thesis, Universitiy of California, San Diego, 2015.

Baumgartner, M., Schilt, A., Eicher, O., Schmitt, J., Schwander, J., Spahni, R., Fischer, H., and Stocker, T. F.: High-resolution interpolar difference of atmospheric methane around the Last Glacial Maximum, Biogeosciences, 9, 3961–3977, doi:10.5194/bg-9-3961-2012, 2012.

Baumgartner, M., Kindler, P., Eicher, O., Floch, G., Schilt, A., Schwander, J., Spahni, R., Capron, E., Chappellaz, J., Leuenberger, M., Fischer, H., and Stocker, T. F.: NGRIP CH_4 concentration from 120 to 10 kyr before present and its relation to a δ^{15}N temperature reconstruction from the same ice core, Climate of the Past, 10, 903–920, doi:10.5194/cp-10-903-2014, 2014.

Bauska, T. K., Joos, F., Mix, A. C., Roth, R., Ahn, J., and Brook, E. J.: Links between atmospheric carbon dioxide, the land carbon reservoir and climate over the past millennium, Nature Geoscience, 8, 383–387, doi:10.1038/ngeo2422, 2015.

Bazin, L., Landais, A., Lemieux-Dudon, B., Toyé Mahamadou Kele, H., Veres, D., Parrenin, F., Martinerie, P., Ritz, C., Capron, E., Lipenkov, V., Loutre, M.-F., Raynaud, D., Vinther, B., Svensson, A., Rasmussen, S. O., Severi, M., Blunier, T., Leuenberger, M., Fischer, H., Masson-Delmotte, V., Chappellaz, J., and Wolff, E.: An optimized multi-proxy, multi-site Antarctic ice and gas orbital chronology (AICC2012): 120–800 ka, Climate of the Past, 9, 1715–1731, doi:10.5194/cp-9-1715-2013, 2013.

Bereiter, B., Lüthi, D., Siegrist, M., Schüpbach, S., Stocker, T. F., and Fischer, H.: Mode change of millennial CO2 variability during the last glacial cycle associated with a bipolar marine carbon seesaw, Proceedings of the National Academy of Sciences, 109, 9755–9760, doi:10.1073/pnas.1204069109, 2012.

Blunier, T. and Brook, E. J.: Timing of millennial-scale climate change in Antarctica and Greenland during the last glacial period, Science, 291, 109–112, 2001.

Bruno, M. and Joos, F.: Terrestrial carbon storage during the past 200 years: A Monte Carlo analysis of CO_2 data from ice core and atmospheric measurements, Global Biogeochemical Cycles, 11, 111–124, 1997.

Buizert, C., Cuffey, K. M., Severinghaus, J. P., Baggenstos, D., Fudge, T. J., Steig, E. J., Markle, B. R., Winstrup, M., Rhodes, R. H., Brook, E. J., Sowers, T. A., Clow, G. D., Cheng, H., Edwards, R. L., Sigl, M., McConnell, J. R., and Taylor, K. C.: The WAIS Divide deep ice core WD2014 chronology – Part 1: Methane synchronization (68-31 ka BP) and the gas age-ice age difference, Climate of the Past, 11, 153–173, doi:10.5194/cp-11-153-2015, 2015.

Chappellaz, J., Stowasser, C., Blunier, T., Baslev-Clausen, D., Brook, E. J., Dallmayr, R., Faïn, X., Lee, J. E., Mitchell, L. E., Pascual, O., Romanini, D., Rosen, J., and Schüpbach, S.: High-resolution glacial and deglacial record of atmospheric methane by continuous-flow and laser spectrometer analysis along the NEEM ice core, Climate of the Past, 9, 2579–2593, doi:10.5194/cp-9-2579-2013, 2013.

Dällenbach, A., Blunier, B., Flückiger, J., Stauffer, B., Chappellaz, J., and Raynaud, D.: Changes in the atmospheric CH_4 gradient between Greenland and Antarctica during the last glacial and the transition to the Holocene, Geophysical Research Letters, 27, 1005–1008, 2000.

Dlugokencky, E., Lang, P., Crotwell, A., Mund, J., Crotwell, M., and Thoning, K.: Atmospheric Methane Dry Air Mole Fractions from the NOAA ESRL Carbon Cycle Cooperative Global Air Sampling Network, 1983-2015, Version: 2016-07-07. Path: ftp://aftp.cmdl.noaa.gov/data/trace_gases/ch4/flask/surface/, 2016a.

Dlugokencky, E., Lang, P., Mund, J., Crotwell, A., Crotwell, M., and Thoning, K.: Atmospheric Carbon Dioxide Dry Air Mole Fractions from the NOAA ESRL Carbon Cycle Cooperative Global Air Sampling Network, 1968-2015, Version: 2016-08-30, Path: ftp://aftp.cmdl.noaa.gov/data/trace_gases/co2/flask/surface/, 2016b.

Enting, I. G.: On the use of smoothing splines to filter CO_2 data, Journal of Geophysical Research: Atmospheres, 92, 10 977–10 984, doi:10.1029/JD092iD09p10977, 1987.

Enting, I. G., Trudinger, C. M., and Etheridge, D. M.: Propoagating data uncertainty through smoothing spline fits, Tellus, 58B, 305–309, doi:10.1111/j.1600-0889.2006.00193.x, 2006.

Etminan, M., Myhre, G., Highwood, E. J., and Shine, K. P.: Radiative forcing of carbon dioxide, methane, and nitrous oxide: A significant revision of the methane radiative forcing, Geophysical Research Letters, 43, 12,614–12,623, doi:10.1002/2016GL071930, 2016.

Flückiger, J., Monnin, E., Stauffer, B., Schwander, J., and Stocker, T. F.: High-resolution Holocene N_2O ice core record and its relationship with CH_4 and CO_2, Global Biogeochemical Cycles, 16, 10.1029/2001GB001 417, doi:10.1029/2001GB001417, 2002.

Flückiger, J., Blunier, T., Stauffer, B., Chappellaz, J., Spahni, R., Kawamura, K., Schwander, J., Stocker, T. F., and Dahl-Jensen, D.: N_2O and CH_4 variations during the last glacial epoch: insights into global processes, Global Biogeochemical Cycles, 18, GB1020, doi: 10.1029/2003GB002 122, 2004.

Hansen, J., Sato, M., Ruedy, R., Nazarenko, L., Lacis, A., Schmidt, G. A., Russell, G., Aleinov, I., Bauer, M., Bauer, S., Bell, N., Cairns, B., Canuto, V., Chandler, M., Cheng, Y., Genio, A. D., Faluvegi, G., Fleming, E., Friend, A., Hall, T., Jackman, C., Kelley, M., Kiang, N., Koch, D., Lean, J., Lerner, J., Lo, K., Menon, S., Miller, R., Minnis, P., Novakov, T., Oinas, V., Perlwitz, J., Perlwitz, J., Rind, D., Romanou, A., Shindell, D., Stone, P., Sun, S., Tausnev, N., Thresher, D., Wielicki, B., Wong, T., Yao, M., and Zhang, S.: Efficacy of climate forcings, Journal of Geophysical Research, 110, D18 104, doi:10.1029/2005JD005776, 2005.

Ivanovic, R. F., Gregoire, L. J., Kageyama, M., Roche, D. M., Valdes, P. J., Burke, A., Drummond, R., Peltier, W. R., and Tarasov, L.: Transient climate simulations of the deglaciation 21–9 thousand years before present (version 1) – PMIP4 Core experiment design and boundary conditions, Geoscientific Model Development, 9, 2563–2587, doi:10.5194/gmd-9-2563-2016, 2016.

Köhler, P., Bintanja, R., Fischer, H., Joos, F., Knutti, R., Lohmann, G., and Masson-Delmotte, V.: What caused Earth's temperature variations during the last 800,000 years? Data-based evidences on radiative forcing and constraints on climate sensitivity, Quaternary Science Reviews, 29, 129–145, doi:10.1016/j.quascirev.2009.09.026, 2010.

Köhler, P., Knorr, G., and Bard, E.: Permafrost thawing as a possible source of abrupt carbon release at the onset of the Bølling/Allerød, Nature Communications, 5, 5520, doi:10.1038/ncomms6520, 2014.

Köhler, P., Völker, C., Knorr, G., and Bard, E.: High Latitude Impacts on Deglacial CO_2: Southern Ocean Westerly Winds and Northern Hemisphere Permafrost Thawing, Nova Acta Leopoldina, 121, 135–140, 2015.

Landais, A., Caillon, N., Goujon, C., Grachev, A. M., Barnola, J. M., Chappellaz, J., Jouzel, J., Masson-Delmotte, V., and Leuenberger, M.: Quantification of rapid temperature change during DO event 12 and phasing with methane inferred from air isotopic measurements, Earth and Planetary Science Letters, 225, 221–232, 2004.

Lewis, S. L. and Maslin, M. A.: Defining the Anthropocene, Nature, 519, 171–180, doi:10.1038/nature14258, 2015.

Loulergue, L., Schilt, A., Spahni, R., Masson-Delmotte, V., Blunier, T., Lemieux, B., Barnola, J.-M., Raynaud, D., Stocker, T. F., and Chappellaz, J.: Orbital and millennial-scale features of atmospheric CH_4 over the past 800,000 years, Nature, 453, 383–386, doi:10.1038/nature06950, 2008.

Lourantou, A., Chappellaz, J., Barnola, J.-M., Masson-Delmotte, V., and Raynaud, D.: Changes in atmospheric CO_2 and its carbon isotopic ratio during the penultimate deglaciation, Quaternary Science Reviews, 29, 1983–1992, doi:10.1016/j.quascirev.2010.05.002, 2010a.

Lourantou, A., Lavrič, J. V., Köhler, P., Barnola, J.-M., Michel, E., Paillard, D., Raynaud, D., and Chappellaz, J.: Constraint of the CO_2 rise by new atmospheric carbon isotopic measurements during the last deglaciation, Global Biogeochemical Cycles, 24, GB2015, doi: 10.1029/2009GB003 545, doi:10.1029/2009GB003545, 2010b.

Lüthi, D., Bereiter, B., Stauffer, B., Winkler, R., Schwander, J., Kindler, P., Leuenberger, M., Kipfstuhl, S., Capron, E., Landais, A., Fischer, H., and Stocker, T. F.: CO2 and O2/N2 variations in and just below the bubble-clathrate transformation zone of Antarctic ice cores, Earth and Planetary Science Letters, 297, 226 – 233, doi:10.1016/j.epsl.2010.06.023, 2010.

MacFarling-Meure, C., Etheridge, D., Trudinger, C., Langenfelds, R., van Ommen, T., Smith, A., and Elkins, J.: Law Dome CO_2, CH_4 and N_2O ice core records extended to 2000 years BP, Geophysical Research Letters, 33, L14 810, doi: 10.1029/2006GL026 152, 2006.

Marcott, S. A., Bauska, T. K., Buizert, C., Steig, E. J., Rosen, J. L., Cuffey, K. M., Fudge, T. J., Severinghaus, J. P., Ahn, J., Kalk, M. L., McConnell, J. R., Sowers, T., Taylor, K. C., White, J. W., and Brook, E. J.: Centennial Scale Changes in the Global Carbon Cycle During the Last Deglaciation, Nature, 514, 616–619, doi:10.1038/nature13799, 2014.

Meinshausen, M., Vogel, E., Nauels, A., Lorbacher, K., Meinshausen, N., Etheridge, D., Fraser, P., Montzka, S. A., Rayner, P., Trudinger, C., Krummel, P., Beyerle, U., Cannadell, J. G., Daniel, J. S., Enting, I., Law, R. M., O'Doherty, S., Prinn, R. G., Reimann, S., Rubino, M., Velders, G. J. M., Vollmer, M. K., and Weiss, R.: Historical greenhouse gas concentrations, Geoscientific Model Development Discussions, 2016, 1–122, doi:10.5194/gmd-2016-169, 2016.

Mitchell, L., Brook, E., Lee, J. E., Buizert, C., and Sowers, T.: Constraints on the Late Holocene Anthropogenic Contribution to the Atmospheric Methane Budget, Science, 342, 964–966, doi:10.1126/science.1238920, 2013.

Mitchell, L. E., Brook, E. J., Sowers, T., McConnell, J. R., and Taylor, K.: Multidecadal variability of atmospheric methane, 1000-1800 C.E., Journal of Geophysical Research, 116, G02 007, doi:10.1029/2010JG001441, 2011.

Monnin, E., Indermühle, A., Dällenbach, A., Flückiger, J., Stauffer, B., Stocker, T. F., Raynaud, D., and Barnola, J.-M.: Atmospheric CO_2 concentrations over the last glacial termination, Science, 291, 112–114, doi:10.1126/science.291.5501.112, 2001.

Monnin, E., Steig, E. J., Siegenthaler, U., Kawamura, K., Schwander, J., Stauffer, B., Stocker, T. F., Morse, D. L., Barnola, J.-M., Bellier, B., Raynaud, D., and Fischer, H.: Evidence for sustantial accumulation rate variability in Antarctica during the Holocene, through synchronization of CO_2 in the Taylor Dome, Dome C and DML ice cores, Earth and Planetary Science Letters, 224, 45–54, 2004.

Myhre, G., Highwood, E. J., Shine, K. P., and Stordal, F.: New estimates of radiative forcing due to well mixed greenhouse gases, Geophysical Research Letters, 25, 2715–2718, 1998.

Otto-Bliesner, B. L., Braconnot, P., Harrison, S. P., Lunt, D. J., Abe-Ouchi, A., Albani, S., Bartlein, P. J., Capron, E., Carlson, A. E., Dutton, A., Fischer, H., Goelzer, H., Govin, A., Haywood, A., Joos, F., Legrande, A. N., Lipscomb, W. H., Lohmann, G., Mahowald, N., Nehrbass-Ahles, C., Pausata, F. S.-R., Peterschmitt, J.-Y., Phipps, S., and Renssen, H.: The PMIP4 contribution to CMIP6 – Part 2: Two Interglacials, Scientific Objective and Experimental Design for Holocene and Last Interglacial Simulations, Geoscientific Model Development Discussions, 2016, 1–36, doi:10.5194/gmd-2016-279, 2016.

Rhodes, R. H., Faïn, X., Stowasser, C., Blunier, T., Chappellaz, J., McConnell, J. R., Romanini, D., Mitchell, L. E., and Brook, E. J.: Continuous methane measurements from a late Holocene Greenland ice core: Atmospheric and in-situ signals, Earth and Planetary Science Letters, 368, 9 – 19, doi:10.1016/j.epsl.2013.02.034, 2013.

Rhodes, R. H., Brook, E. J., Chiang, J. C. H., Blunier, T., Maselli, O. J., McConnell, J. R., Romanini, D., and Severinghaus, J. P.: Enhanced tropical methane production in response to iceberg discharge in the North Atlantic, Science, 348, 1016–1019, doi:10.1126/science.1262005, 2015.

Rubino, M., Etheridge, D. M., Trudinger, C. M., Allison, C. E., Battle, M. O., Langenfelds, R. L., Steele, L. P., Curran, M., Bender, M., White, J. W. C., Jenk, T. M., Blunier, T., and Francey, R. J.: A revised 1000-year atmospheric δ^{13}C-CO_2 record from Law Dome and South Pole, Antarctica, Journal of Geophysical Research: Atmospheres, 118, 8482–8499, doi:10.1002/jgrd.50668, 2013.

Schilt, A., Baumgartner, M., Blunier, T., Schwander, J., Spahni, R., Fischer, H., and Stocker, T. F.: Glacial-interglacial and millennial-scale variations in the atmospheric nitrous oxide concentration during the last 800 000 years, Quaternary Science Reviews, 29, 182–192, doi:10.1016/j.quascirev.2009.03.011, 2010a.

Schilt, A., Baumgartner, M., Schwander, J., Buiron, D., Capron, E., Chappellaz, J., Loulergue, L., Schüpbach, S., Spahni, R., Fischer, H., and Stocker, T. F.: Atmospheric nitrous oxide during the last 140,000 years, Earth and Planetary Science Letters, 300, 33 – 43, doi:10.1016/j.epsl.2010.09.027, 2010b.

Schilt, A., Baumgartner, M., Eicher, O., Chappellaz, J., Schwander, J., Fischer, H., and Stocker, T. F.: The response of atmospheric nitrous oxide to climate variations during the last glacial period, Geophysical Research Letters, 40, 1888–1893, doi:10.1002/grl.50380, 2013.

Schilt, A., Brook, E. J., Bauska, T. K., Baggenstos, D., Fischer, H., Joos, F., Petrenko, V. V., Schaefer, H., Schmitt, J., Severinghaus, J. P., Spahni, R., and Stocker, T. F.: Isotopic constraints on marine and terrestrial N2O emissions during the last deglaciation, Nature, 516, 234–237, doi:10.1038/nature13971, 2014.

Schmitt, J., Schneider, R., Elsig, J., Leuenberger, D., Lourantou, A., Chappellaz, J., Köhler, P., Joos, F., Stocker, T. F., Leuenberger, M., and Fischer, H.: Carbon isotope constraints on the deglacial CO_2 rise from ice cores, Science, 336, 711–714, doi:10.1126/science.1217161, 2012.

Schneider, R., Schmitt, J., Köhler, P., Joos, F., and Fischer, H.: A reconstrution of atmospheric carbon dioxide and its stable carbon isotopic composition from the penultimate glacial maximum to the last glacial inception, Climate of the Past, 9, 2507—2523, doi:10.5194/cp-9-2507-2013, 2013.

Schüpbach, S., Federer, U., Kaufmann, P. R., Hutterli, M. A., Buiron, D., Blunier, T., Fischer, H., and Stocker, T. F.: A New Method for High-Resolution Methane Measurements on Polar Ice Cores Using Continuous Flow Analysis, Environmental Science & Technology, 43, 5371–5376, doi:10.1021/es9003137, 2009.

Sigl, M., Fudge, T. J., Winstrup, M., Cole-Dai, J., Ferris, D., McConnell, J. R., Taylor, K. C., Welten, K. C., Woodruff, T. E., Adolphi, F., Bisiaux, M., Brook, E. J., Buizert, C., Caffee, M. W., Dunbar, N. W., Edwards, R., Geng, L., Iverson, N., Koffman, B., Layman, L., Maselli, O. J., McGwire, K., Muscheler, R., Nishiizumi, K., Pasteris, D. R., Rhodes, R. H., and Sowers, T. A.: The WAIS Divide deep ice core WD2014 chronology - Part 2: Annual-layer counting (0-31 ka BP), Climate of the Past, 12, 769–786, doi:10.5194/cp-12-769-2016, 2016.

Spahni, R., Chappellaz, J., Stocker, T. F., Loulergue, L., Hausammann, G., Kawamura, K., Flückiger, J., Schwander, J., Raynaud, D., Masson-Delmotte, V., and Jouzel, J.: Atmospheric methane and nitrous oxide of the late Pleistocene from Antarctic ice cores, Science, 310, 1317–1321, doi: 10.1126/science.1120 132, 2005.

Stauffer, B., Blunier, T., Dällenbach, A., Indermühle, A., Schwander, J., Stocker, T. F., Tschumi, J., Chappellaz, J., Raynaud, D., Hammer, C. U., and Claussen, H. B.: Atmospheric CO_2 concentration and millennial-scale climate change during the last glacial period, Nature, 392, 59–62, 1998.

Stauffer, B., Flückiger, J., Monnin, E., Schwander, J., Barnola, J.-M., and Chappellaz, J.: Atmospheric CO_2, CH_4 and N_2O records over the past 60000 years based on the comparison of different polar ice cores, Annals of Glaciology, 35, 202–208, 2002.

Steffen, W., Leinfelder, R., Zalasiewicz, J., Waters, C. N., Williams, M., Summerhayes, C., Barnosky, A. D., Cearreta, A., Crutzen, P., Edgeworth, M., Ellis, E. C., Fairchild, I. J., Galuszka, A., Grinevald, J., Haywood, A., Ivar do Sul, J., Jeandel, C., McNeill, J., Odada, E., Oreskes, N., Revkin, A., Richter, D. d., Syvitski, J., Vidas, D., Wagreich, M., Wing, S. L., Wolfe, A. P., and Schellnhuber, H.: Stratigraphic and Earth System approaches to defining the Anthropocene, Earth's Future, pp. n/a–n/a, doi:10.1002/2016EF000379, 2016.

Veres, D., Bazin, L., Landais, A., Toyé Mahamadou Kele, H., Lemieux-Dudon, B., Parrenin, F., Martinerie, P., Blayo, E., Blunier, T., Capron, E., Chappellaz, J., Rasmussen, S. O., Severi, M., Svensson, A., Vinther, B., and Wolff, E. W.: The Antarctic ice core chronology (AICC2012): an optimized multi-parameter and multi-site dating approach for the last 120 thousand years, Climate of the Past, 9, 1733–1748, doi:10.5194/cp-9-1733-2013, 2013.

WAIS Divide Project Members: Precise interpolar phasing of abrupt climate change during the last ice age, Nature, 520, 661–665, doi:10.1038/nature14401, 2015.

Williams, M., Zalasiewicz, J., Waters, C. N., Edgeworth, M., Bennett, C., Barnosky, A. D., Ellis, E. C., Ellis, M. A., Cearreta, A., Haff, P. K., Ivar do Sul, J. A., Leinfelder, R., McNeill, J. R., Odada, E., Oreskes, N., Revkin, A., Richter, D. d., Steffen, W., Summerhayes, C., Syvitski, J. P., Vidas, D., Wagreich, M., Wing, S. L., Wolfe, A. P., and Zhisheng, A.: The Anthropocene: a conspicuous stratigraphical signal of anthropogenic changes in production and consumption across the biosphere, Earth's Future, 4, 34–53, doi:10.1002/2015EF000339, 2016.

Earth Syst. Sci. Data Discuss., doi:10.5194/essd-2017-6, 2017
Manuscript under review for journal Earth Syst. Sci. Data
Discussion started: 20 February 2017

Table 1. Locations of the different data sources, ordered north to south. Individual sites of the NOAA oberservational network are not explicitly mentioned here, when they only contribute to global mean calculations. SH CH_4: Southern Hermisphere CH_4.

Site	Latitude	Longitude	Data used here
NGRIP	75.10° North	42.32° West	N_2O
GRIP	72.583° North	37.633° West	comparing to SH CH_4
Barrow	71.3230° North	156.6114° West	comparing to SH CH_4
Mauna Loa	19.5362° North	155.5763° West	CO_2
Law Dome[1]	∼66.73° South	∼112.83° East	CO_2, SH CH_4, N_2O
Talos Dome (TALDICE)	72.817° South	159.183° East	CO_2, N_2O
EPICA Dronning Maud Land (EDML)	75.0° South	0.067° East	CO_2
EPICA Dome C (EDC)	75.1° South	123.35° East	CO_2, SH CH_4, N_2O
Taylor Glacier[2]	∼77.77° South	∼161.7° East	N_2O
WAIS Divide Ice Core (WDC)	79.468° South	112.086° West	CO_2, CH_4
Siple Dome	81.66° South	148.82° West	CO_2
South Pole[1]	90° South	59° East	CO_2, SH CH_4

Notes:

1: The data compilation of MacFarling-Meure et al. (2006); Rubino et al. (2013) on CO_2, SH CH_4, and N_2O uses data from the Law Dome deep ice core and from various shallow ice and firn core in its vicinity, but also from atmospheric data from Cape Grim and firn core data from South Pole. While we here state all the relevant positions, the original source of the individual data points is not marked in Tables 2, 5 and 7, or in the data files uploaded to PANGAEA, but then only labeled with "Law Dome" as data source. Please see the original reference for further details.

2: Data taken from Taylor Glacier are based on a "horizontal ice core", which has not a point location as all other sites.

Earth Syst. Sci. Data Discuss., doi:10.5194/essd-2017-6, 2017
Manuscript under review for journal Earth Syst. Sci. Data
Discussion started: 20 February 2017

Open Access Earth System Science Data Discussions

Table 2. Data used to construct the CO_2 spline.

Time (in BP)	Time (in CE)	Source	Age scale	Citation
–66 to –8	2016 to 1958	Mauna Loa[1] (monthly)	—	Dlugokencky et al. (2016b)
–10 to 1949	1960 to 1	Law Dome[2]	as in refs.	MacFarling-Meure et al. (2006); Rubino et al. (2013)
200 to 1210	1750 to 740	WDC[3]	WD2014	Ahn et al. (2012); Bauska et al. (2015)
1902 to 10954	48 to before CE	EDC[4]	AICC2012	Monnin et al. (2001, 2004)
8807 to 22909	—	WDC	WD2014	Marcott et al. (2014); Buizert et al. (2015); Sigl et al. (2016)
21926 to 48720	—	Siple Dome	GICC05	Ahn and Brook (2014)
38127 to 69672	—	Talos Dome[5]	AICC2012	Bereiter et al. (2012)
43205 to 113429	—	EDML	AICC2012	Bereiter et al. (2012); Lüthi et al. (2010)
104331 to 156307	—	EDC	AICC2012	Schneider et al. (2013)
124859 to 153135	—	EDC	AICC2012	Lourantou et al. (2010a)

Notes:

1: Data taken from ftp://aftp.cmdl.noaa.gov/products/trends/co2/co2_mm_mlo.txt.

2: Law Dome data are taken from various sources, see references for details. They are available from 2001 CE to 1 CE, only data before 1960 CE are taken for the spline.

3: WDC data are available 10 BP to 1217 BP, but not all were used here.

4: EDC data are available 350 BP to 22236 BP, but not all were used here.

5: Talos Dome data exist from 34360 BP, but contains some outliers before 38 kyr BP.

Earth Syst. Sci. Data Discuss., doi:10.5194/essd-2017-6, 2017
Manuscript under review for journal Earth Syst. Sci. Data
Discussion started: 20 February 2017

Table 3. Statistics of the CO_2 spline. Interval i_{CO_2}; s: scaling factor to fulfil the constrains given by the prescribed P_{cutoff}; $\overline{P_{\mathrm{cutoff}}}$: average realised cutoff period. Δt: mean data spacing; v: mean 1σ error; exact time framing is given by the age of the first (t_{start}) and last (t_{stop}) data point of the interval (in years BP); N: number of data points within interval. In the last column the underlying data source is briefly mentioned, see Table 2 for details and citations.

i_{CO_2}	s	P_{cutoff}	$\overline{P_{\mathrm{cutoff}}}$	Δt	v	t_{start}	t_{stop}	N	Data source
	-	yr	yr	yr	ppm	yr BP	yr BP	-	
1	1.00	4.0	4.0	0.1	0.3	-66.0	-8.1	699	Mauna Loa, Law Dome
2	2.65	20.0	18.5	0.4	1.3	-8.0	19.2	69	Law Dome
3	7.49	40.0	37.5	1.0	1.2	20.6	117.1	96	Law Dome
4	79.91	160.0	151.0	4.3	0.9	123.1	997.8	206	Law Dome, WDC
5	388.87	500.0	468.8	13.0	1.0	1006.0	1796.5	62	Law Dome, WDC
6	5377.63	3000.0	2883.1	93.3	1.0	1814.0	8994.9	78	Law Dome, WDC, EDC
7	1532.28	1600.0	1519.4	48.8	1.3	9060.2	10962.5	40	WDC, EDC
8	357.66	600.0	567.4	28.1	1.0	11060.3	18463.6	264	WDC
9	1563.85	2000.0	1806.4	176.2	1.1	18559.8	109840.0	519	WDC, Siple D, Talos D, EDML, EDC
10	1690.90	3000.0	2593.3	383.9	1.5	110555.4	127829.0	46	EDML, EDC
11	225.60	1000.0	921.5	257.3	1.5	128024.5	134970.7	28	EDC
12	530.27	2000.0	1853.3	871.7	1.4	135387.0	156306.8	25	EDC

Table 4. Comparison of our final spline data with values used for PMIP4 experiments for 21 kyr (Ivanovic et al., 2016) and 1850 CE, 6 kyr, 127 kyr (Otto-Bliesner et al., 2016). Please be aware that the PMIP4 values should be millennial-scale mean numbers to serve as forcing values for time slice experiments, while the values depicted from this study are snapshots of the given points in time. Furthermore, we calculate SH CH_4 values, while in PMIP4 the global CH_4 is given.

GHG	Unit	1850 CE	6 kyr	21 kyr	127 kyr
This study:					
CO_2	ppm	286.1	264.4	187	274
SH CH_4	ppb	795	553	382	660
N_2O	ppb	271	261	206	257
PMIP4:					
CO_2	ppm	284.3[1]	264.4	190	275
global CH_4	ppb	808	597	375	685
N_2O	ppb	273	262	200	255

Note:

1: In the discussion version of this paper a value of 284.6 ppm was given, which has been revised to the here stated value of 284.3 ppm.

Earth Syst. Sci. Data Discuss., doi:10.5194/essd-2017-6, 2017
Manuscript under review for journal Earth Syst. Sci. Data
Discussion started: 20 February 2017

Open Access Earth System Science Data Discussions

Table 5. Data used to construct (or compare to) the Southern Hemisphere CH_4 spline.

Time (in BP)	Time (in CE)	Source	Age scale	Spline[5]	Citation
–66 to –34	2016 to 1984	NOAA network[1] (annual)	—	no	Dlugokencky et al. (2016a)
–66 to –33	2016 to 1983	South Pole[2] (monthly)	—	yes	Dlugokencky et al. (2016a)
–66 to –33	2016 to 1983	Barrow[3] (monthly)	—	no	Dlugokencky et al. (2016a)
–32 to 168	1982 to 1782	Law Dome[4]	as in refs.	yes	MacFarling-Meure et al. (2006); Rubino et al. (2013)
169 to 67145	1781 to before CE	WDC	WD2014	yes	WAIS Divide Project Members (2015); Marcott et al. (2014); Buizert et al. (2015); Mitchell et al. (2013, 2011); Sigl et al. (2016)
192 to 100469	1758 to before CE	GRIP	GICC05ext	no	Blunier and Brook (2001); Dällenbach et al. (2000); Flückiger et al. (2004); Landais et al. (2004)
67401 to 156211	—	EDC	AICC2012	yes	Loulergue et al. (2008)

Notes:

1: Global annual mean of the NOAA network. Data taken from ftp://aftp.cmdl.noaa.gov/products/trends/ch4/ch4_annmean_gl.txt.

2: Data taken from ftp://aftp.cmdl.noaa.gov/data/trace_gases/ch4/flask/surface/ch4_spo_surface-flask_1_ccgg_month.txt

3: Data taken from ftp://aftp.cmdl.noaa.gov/data/trace_gases/ch4/flask/surface/ch4_brw_surface-flask_1_ccgg_month.txt

4: Law Dome data are taken from various sources, see references for details. They exist for 2005 CE to 14 CE (or –55 BP to 1936 BP), but only the part bridging the gap between instrumental data and WDC are taken for the calculation of the spline (1982 CE to 1782 CE or –32 BP to 168 BP).

5: Indicates if the data are used to construct the spline.

Earth Syst. Sci. Data Discuss., doi:10.5194/essd-2017-6, 2017
Manuscript under review for journal Earth Syst. Sci. Data
Discussion started: 20 February 2017

Table 6. Statistics of the CH_4 spline. Interval i_{CH_4}; s: scaling factor to fulfil the constrains given by the prescribed P_{cutoff}; $\overline{P_{cutoff}}$: average realised cutoff period. Δt: mean data spacing; v: mean 1σ error; exact time framing is given by the age of the first (t_{start}) and last (t_{stop}) data point of the interval (in years BP); N: number of data points within interval. In the last column the underlying data source is briefly mentioned, see Table 5 for details and citations.

i_{CH_4}	s	P_{cutoff}	$\overline{P_{cutoff}}$	Δt	v	t_{start}	t_{stop}	N	Data source
	-	yr	yr	yr	ppb	yr BP	yr BP	-	
1	1.00	4.0	4.0	0.1	2.0	-66.0	-33.1	396	South Pole
2	0.68	10.0	9.5	1.7	4.0	-31.8	165.1	114	Law Dome
3	2.10	20.0	19.9	8.2	2.4	169.0	2591.0	296	WDC
4	7.71	50.0	49.1	23.7	2.4	2602.0	6496.0	165	WDC
5	5.79	40.0	39.6	17.3	2.4	6509.0	16978.0	607	WDC
6	9.85	60.0	59.2	30.2	2.4	17001.0	22768.0	192	WDC
7	89.53	200.0	195.9	45.1	2.4	22804.0	59991.0	825	WDC
8	69.49	500.0	488.8	232.1	8.5	60058.0	127831.0	293	WDC, EDC
9	171.96	1000.0	982.0	440.4	10.0	128026.0	156211.0	65	EDC

Earth Syst. Sci. Data Discuss., doi:10.5194/essd-2017-6, 2017
Manuscript under review for journal Earth Syst. Sci. Data
Discussion started: 20 February 2017

Open Access Earth System Science Data Discussions

Table 7. Data used to construct the N_2O spline.

Time (in BP)	Time (in CE)	Source	Age scale	Citation
–66 to –49	2016 to 1999	NOAA network (monthly)	—	Nitrous Oxide data from the NOAA/ESRL halocarbons in situ program[1]
–50 to –38	2000 to 1988	NOAA network (monthly)	—	RITS Nitrous Oxide data from the NOAA/ESRL halocarbons program[2]
–33 to 1937	1983 to 13	Law Dome[3]	as in refs.	MacFarling-Meure et al. (2006)
1975 to 11502	—	EDC[4]	AICC2012	Flückiger et al. (2002); Stauffer et al. (2002)
29065 to 134519	—	EDC	AICC2012	Spahni et al. (2005)
9858 to 15843	—	Taylor Glacier	WD2014[5]	Schilt et al. (2014)
15000 to 118602	—	NGRIP[6]	AICC2012	Flückiger et al. (2004); Schilt et al. (2010b, 2013)
15000 to 134418	—	Talos Dome[7]	AICC2012	Schilt et al. (2010b)

Notes:

1: ftp://ftp.cmdl.noaa.gov/hats/n2o/insituGCs/CATS/global/insitu_global_N2O.txt.

2: ftp://ftp.cmdl.noaa.gov/hats/n2o/insituGCs/RITS/global/RITS_global_N2O.txt.

3: Law Dome data are taken from various sources, see references for details. They exist from 2004 CE to 13 CE (or –54 BP to 1937 BP), but only those older than the instrumental record (1986 CE and older) are taken here.

4: Data exist from 334 BP (or 1616 CE) until 11502 BP, but only data not yet covered by the Law Dome records (13 CE or 1937 BP and older) are considered here.

5: WD2014 age model for Taylor Glacier, published in Baggenstos (2015).

6: Data exit for 11068 BP – 119555 BP, but only those before 15 kyr BP are considered here. Five data points in the oldest part considerably disagree from SH records and are therefore rejected.

7: Data exit for 217 BP – 134418 BP, but only those before 15 kyr BP are considered here.

Earth Syst. Sci. Data Discuss., doi:10.5194/essd-2017-6, 2017
Manuscript under review for journal Earth Syst. Sci. Data
Discussion started: 20 February 2017

Open Access Earth System Science Data Discussions

Table 8. Statistics of N_2O spline. Interval i_{N_2O}; s: scaling factor to fulfil the constrains given by the prescribed $P_{\rm cutoff}$; $\overline{P_{\rm cutoff}}$: average realised cutoff period. Δt: mean data spacing; v: mean 1σ error; exact time framing is given by the age of the first ($t_{\rm start}$) and last ($t_{\rm stop}$) data point of the interval (in years BP); N: number of data points within interval. In the last column the underlying data source is briefly mentioned, see Table 7 for details and citations.

i_{N_2O}	s	$P_{\rm cutoff}$	$\overline{P_{\rm cutoff}}$	Δt	v	$t_{\rm start}$	$t_{\rm stop}$	N	Data source
	-	yr	yr	yr	ppb	yr BP	yr BP	-	
1	1.00	4.0	3.4	0.1	0.8	-66.0	-38.3	334	NOAA network
2	3.01	50.0	48.7	2.5	7.2	-33.7	95.0	53	Law Dome
3	19.08	200.0	190.2	16.8	7.0	104.0	389.6	18	Law Dome
4	321.85	1000.0	952.4	85.1	4.6	400.3	9425.6	107	Law Dome, EDC
5	77.33	500.0	469.0	58.2	5.8	9517.2	15974.7	112	EDC, Taylor Glacier, NGRIP, Talos D.
6	1443.10	2000.0	1915.3	60.4	4.9	16003.0	116900.0	1672	EDC, NGRIP, Talos D.
7	4236.11	5000.0	4792.5	370.0	4.2	117130.0	134519.0	48	EDC, NGRIP, Talos D.

Earth Syst. Sci. Data Discuss., doi:10.5194/essd-2017-6, 2017
Manuscript under review for journal Earth Syst. Sci. Data
Discussion started: 20 February 2017

Open Access Earth System Science Data Discussions

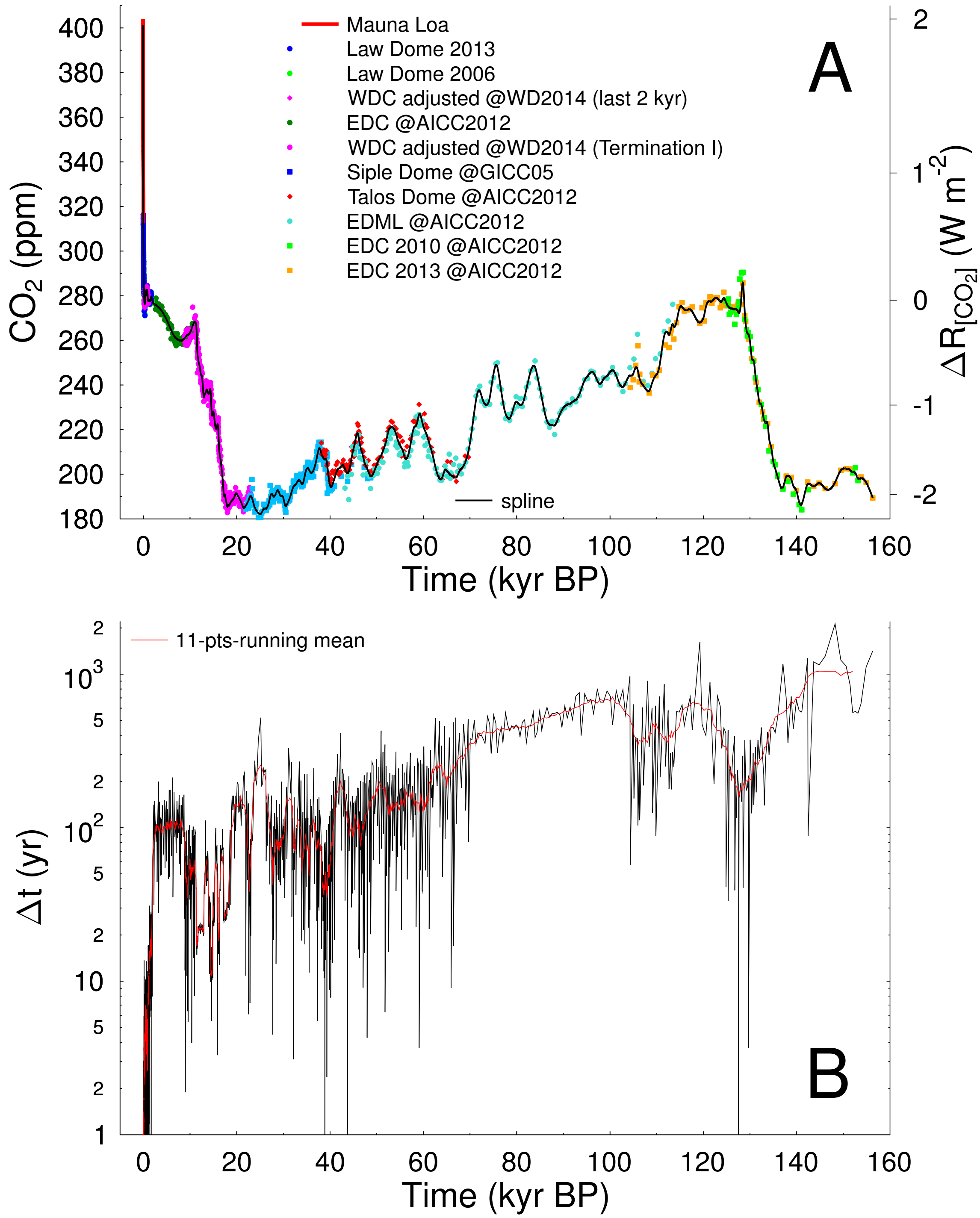

Figure 1. CO_2 spline covering all data: 2016 CE – 156,307 BP. WDC data have been adjusted to reduce offsets, see text for details. In (A) the right axis contains the resulting radiative forcing $\Delta R_{[CO_2]} = 5.35 \cdot ln(CO_2/(278\text{ ppm}))$ W m^{-2} calculated after Myhre et al. (1998). (B) Age distance (Δt) of the CO_2 data points underlying the spline on a log-scale.

Earth Syst. Sci. Data Discuss., doi:10.5194/essd-2017-6, 2017
Manuscript under review for journal Earth Syst. Sci. Data
Discussion started: 20 February 2017

Open Access Earth System Science Data Discussions

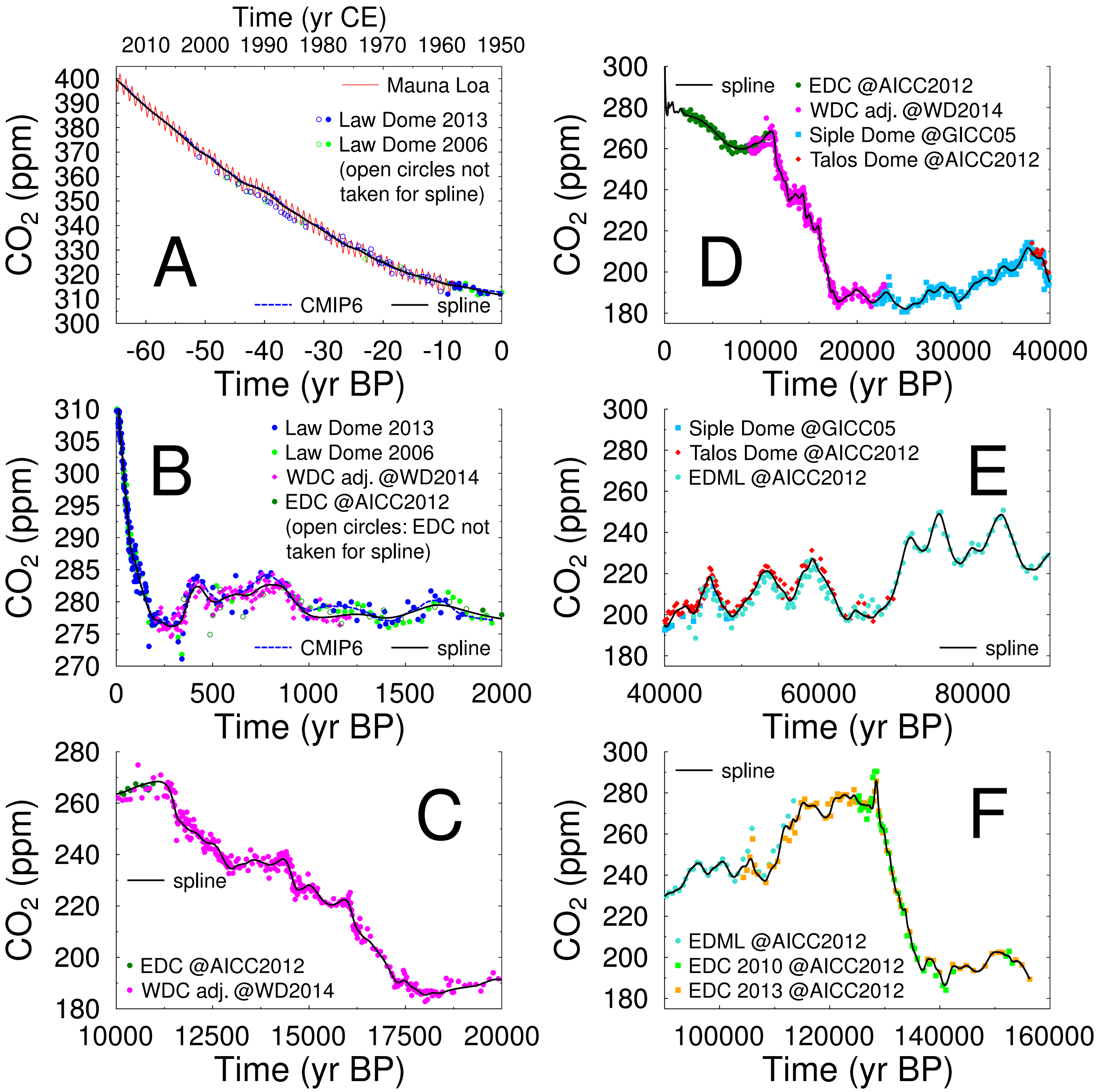

Figure 2. Details of the CO_2 spline. (A) instrumental times (1950–2016 CE); (B) 0–2000 BP; (C) Termination I; (D) 0–40 kyr BP; (E) 40–90 kyr BP; (F) 90–160 kyr BP. WDC data have been adjusted to reduce offsets, see text for details. Dashed line labeled CMIP6 in subfigures A,B is the compiled CO_2 record to be used in CMIP6 experiments for the last 2 kyr (Meinshausen et al., 2016).

Earth Syst. Sci. Data Discuss., doi:10.5194/essd-2017-6, 2017
Manuscript under review for journal Earth Syst. Sci. Data
Discussion started: 20 February 2017

Open Access Earth System Science Data Discussions

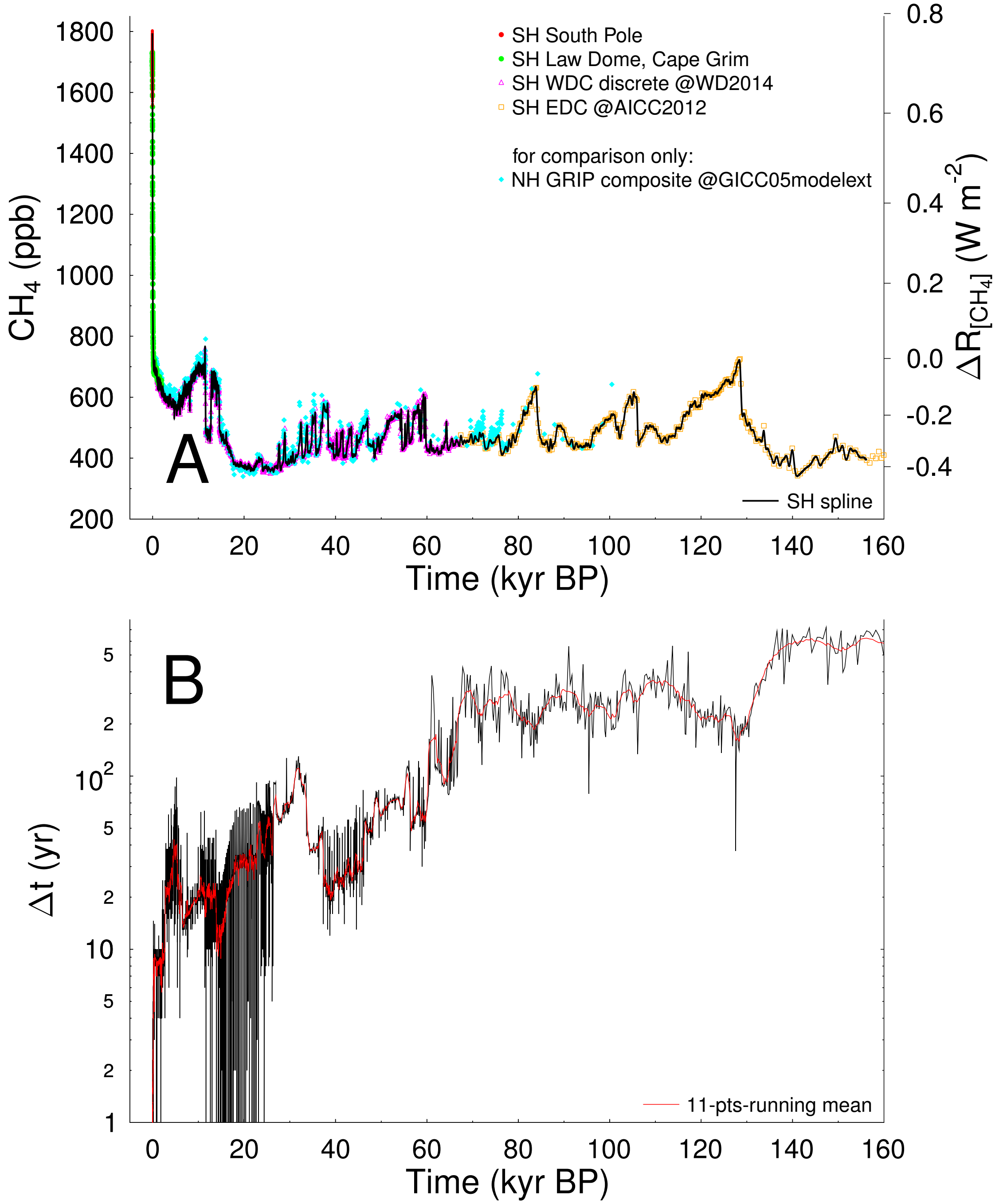

Figure 3. CH_4 spline covering all data: 2016 CE – 156,211 BP. Details on plotted data are explained in the text. In (A) the right axis contains the resulting radiative forcing approximated with $\Delta R_{[CH_4]} \sim 1.4 \cdot 0.036 \cdot (\sqrt{CH_4/ppb} - \sqrt{742})$ W m^{-2} based on Myhre et al. (1998), but neglecting interacting effects of CH_4 and N_2O, and considering indirect effects of CH_4 on stratospheric H_2O and tropospheric O_3 (Hansen et al., 2005; Köhler et al., 2010). Latitudinal origin of data is indicated by NH and SH, implying northern and southern hemisphere, respectively. (B) Age distance (Δt) of the CH_4 data points underlying the spline on a log-scale.

Earth Syst. Sci. Data Discuss., doi:10.5194/essd-2017-6, 2017
Manuscript under review for journal Earth Syst. Sci. Data
Discussion started: 20 February 2017

Open Access Earth System Science Data Discussions

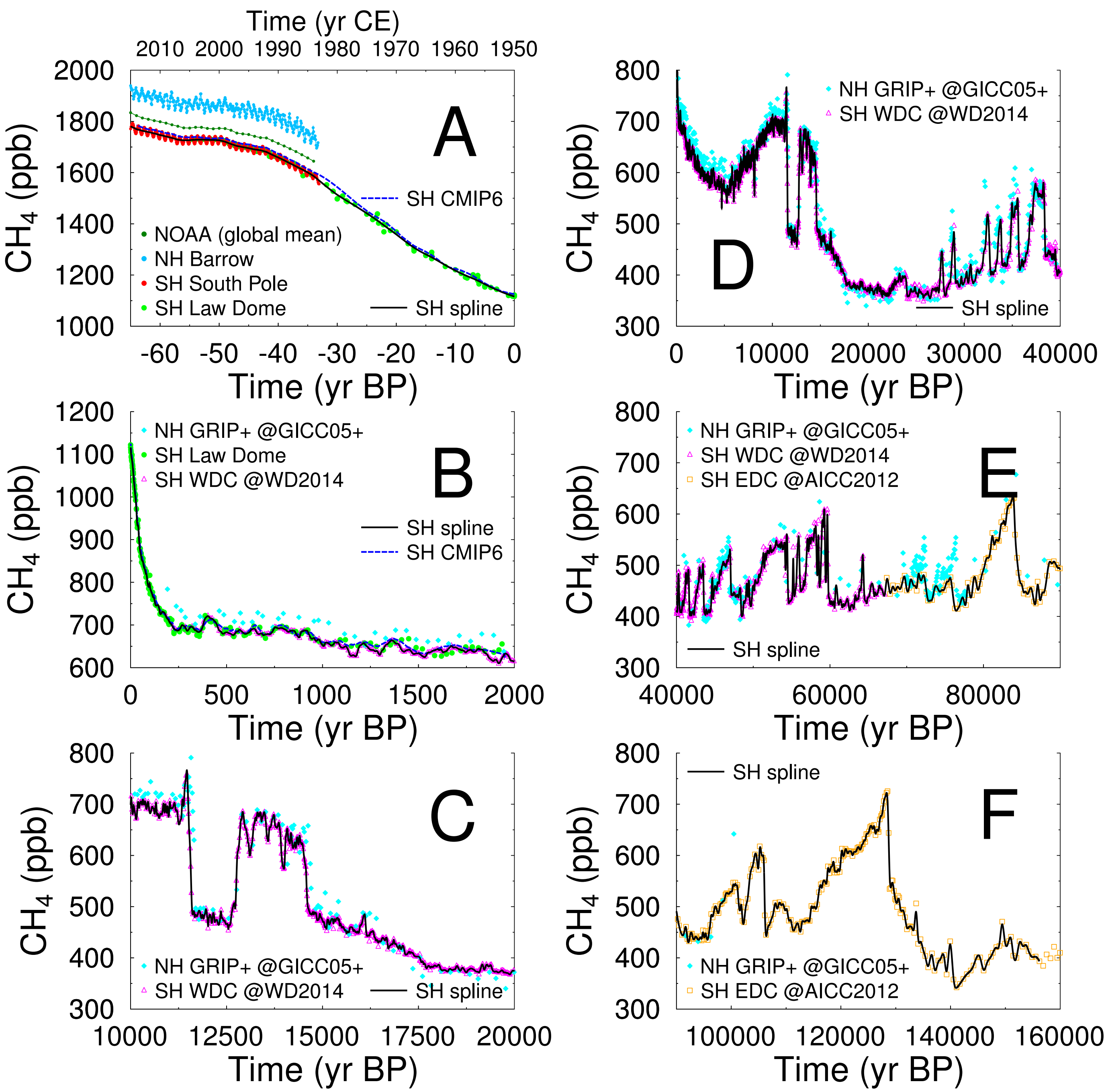

Figure 4. Details of the southern hemispheric CH_4 spline. (A) instrumental times (1950–2016 CE); (B) 0–2000 BP; (C) Termination I; (D) 0–40 kyr BP; (E) 40–90 kyr BP; (F) 90–160 kyr BP. Hemispheric origin of data is indicated by NH (north) and SH (south). From WDC the discrete data have been plotted. GRIP+: Greenland composite; GICC05+: GICC05 model extended. See text for details. Dashed line labeled CMIP6 in subfigures A,B is the compiled CH_4 record to be used in CMIP6 experiments for the last 2 kyr (Meinshausen et al., 2016).

Earth Syst. Sci. Data Discuss., doi:10.5194/essd-2017-6, 2017
Manuscript under review for journal Earth Syst. Sci. Data
Discussion started: 20 February 2017

Open Access Earth System Science Data Discussions

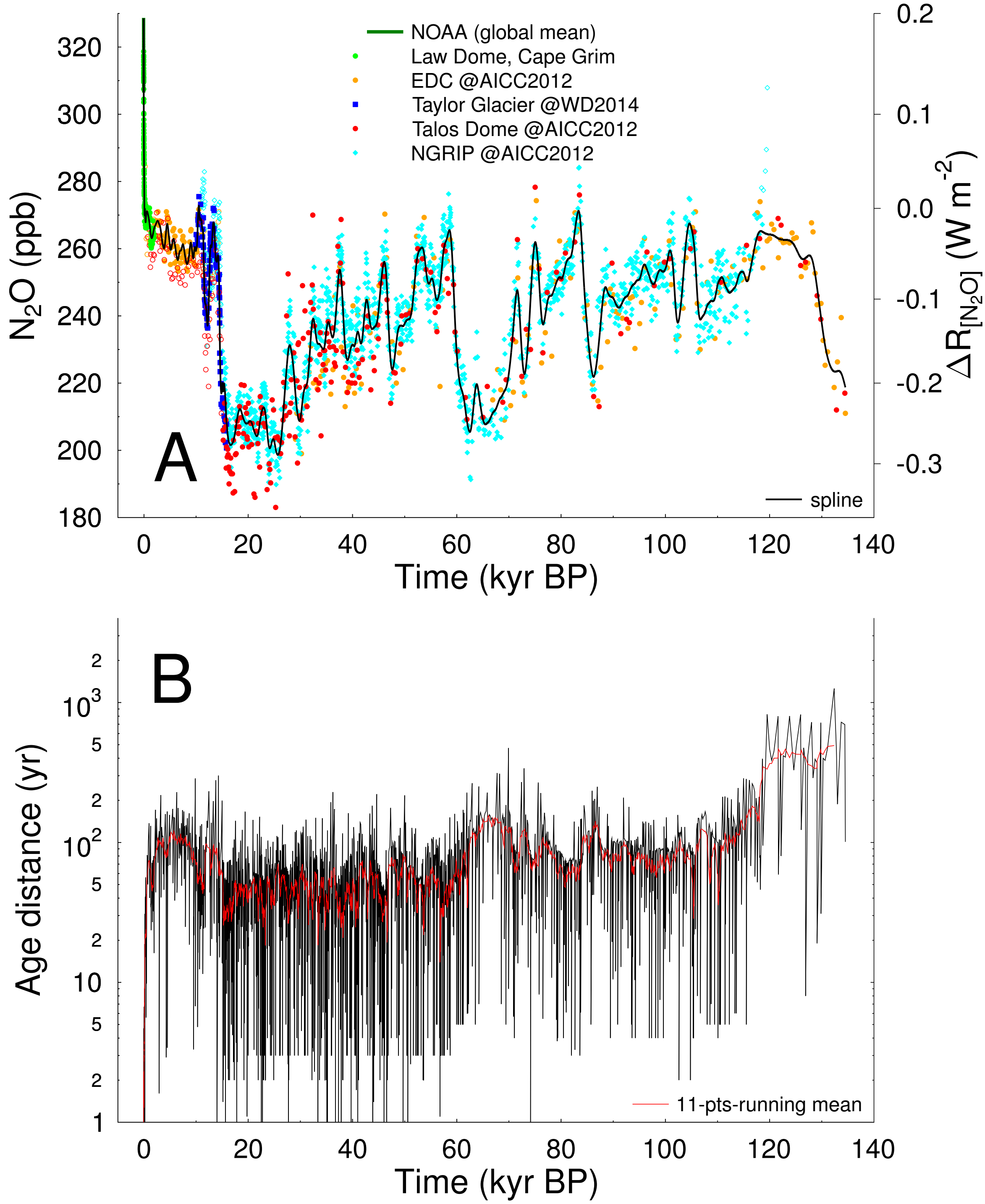

Figure 5. N_2O spline covering all data: 2016 CE – 134,519 BP. Details on plotted data are explained in the text. In (A) the right axis contains the resulting radiative forcing approximated with $\Delta R_{[N_2O]} \sim 0.12 \cdot (\sqrt{N_2O/\mathrm{ppb}} - \sqrt{272})$ W m^{-2} after Myhre et al. (1998), neglecting interacting effects of CH_4 and N_2O. Filled symbols: data taken for spline; open symbols: data not taken for spline. (B) Age distance (Δt) of the N_2O data points underlying the spline on a log-scale.

Earth Syst. Sci. Data Discuss., doi:10.5194/essd-2017-6, 2017
Manuscript under review for journal Earth Syst. Sci. Data
Discussion started: 20 February 2017

Open Access Earth System Science Data Discussions

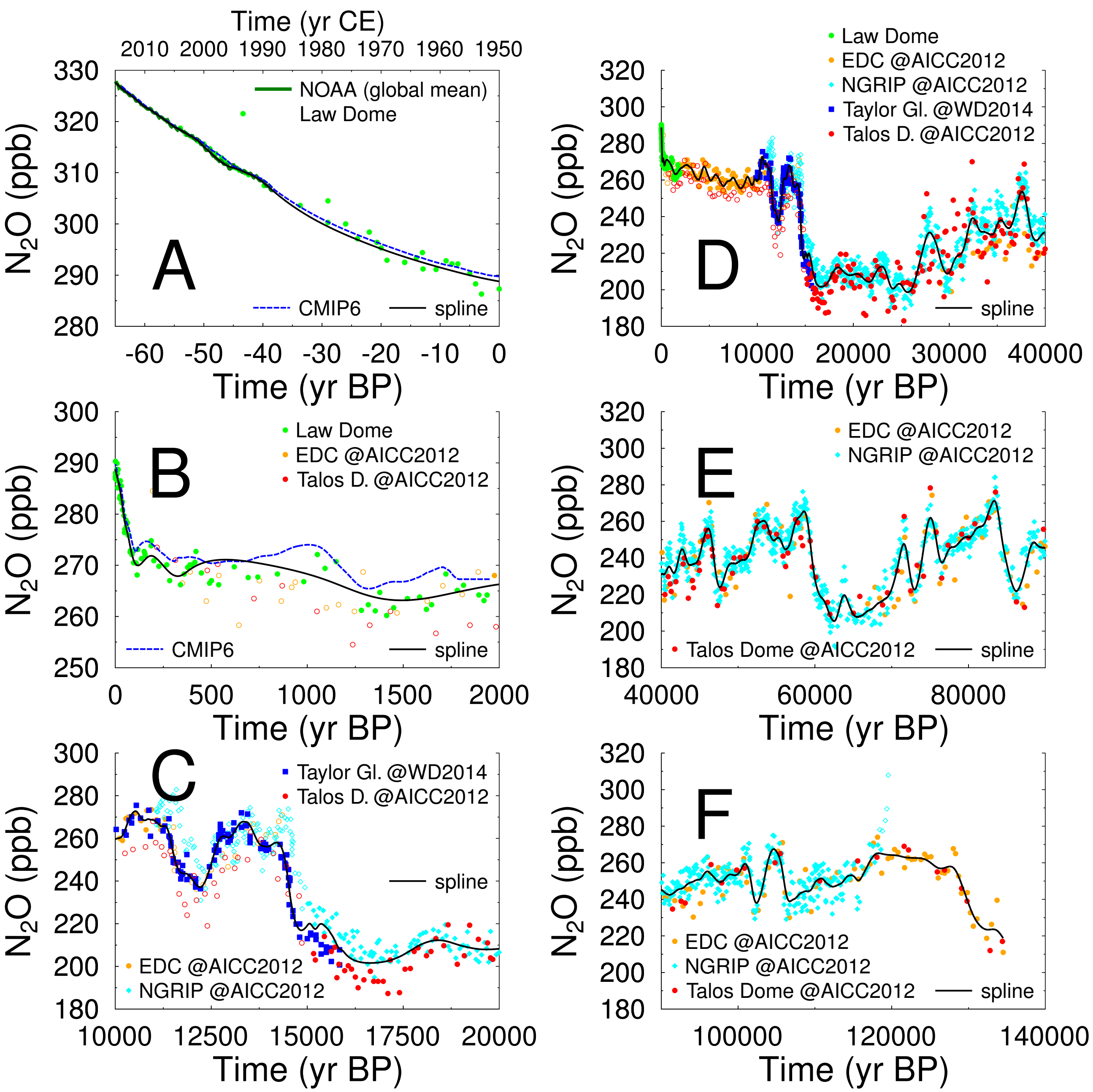

Figure 6. Details of the N_2O spline. (A) instrumental times (1950–2016 CE); (B) 0–2000 BP; (C) Termination I; (D) 0–40 kyr BP; (E) 40–90 kyr BP; (F) 90–140 kyr BP. Filled symbols: data taken for spline; open symbols: data not taken for spline. See text for further details. Dashed line labeled CMIP6 in subfigures A,B is the compiled N_2O record to be used in CMIP6 experiments for the last 2 kyr (Meinshausen et al., 2016).

Open Access Earth System Science Data Discussions

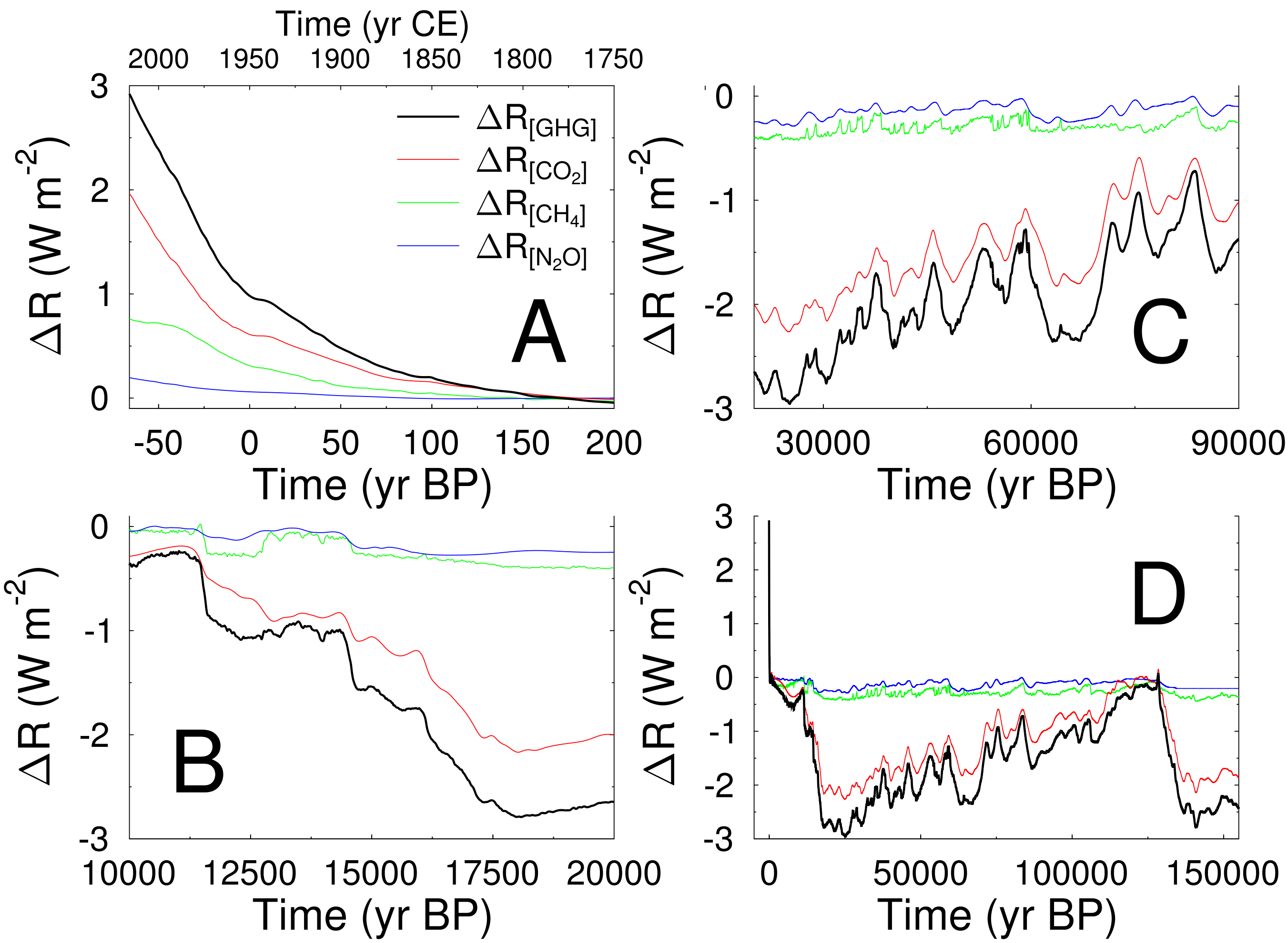

Figure 7. Calculated radiative forcing of CO_2, CH_4, N_2O, and of their sum ($\Delta R_{[GHG]}$). The calculations are based on the Eqns. 5-7 given in the text (following Myhre et al., 1998). Sub-panels focus on specific time windows: (A) Anthropogenic rise since 1750 CE; (B) Termination I; (C) 20-90 kyr BP including the abrupt changes during D/O event; (D) Full record from 2016 CE to 156 kyr BP, here N_2O was kept constant beyond 134 kyr BP.

Earth Syst. Sci. Data Discuss., doi:10.5194/essd-2017-6, 2017
Manuscript under review for journal Earth Syst. Sci. Data
Discussion started: 20 February 2017

Open Access Earth System Science Data Discussions

Appendix Figures

Earth Syst. Sci. Data Discuss., doi:10.5194/essd-2017-6, 2017
Manuscript under review for journal Earth Syst. Sci. Data
Discussion started: 20 February 2017

Open Access Earth System Science Data Discussions

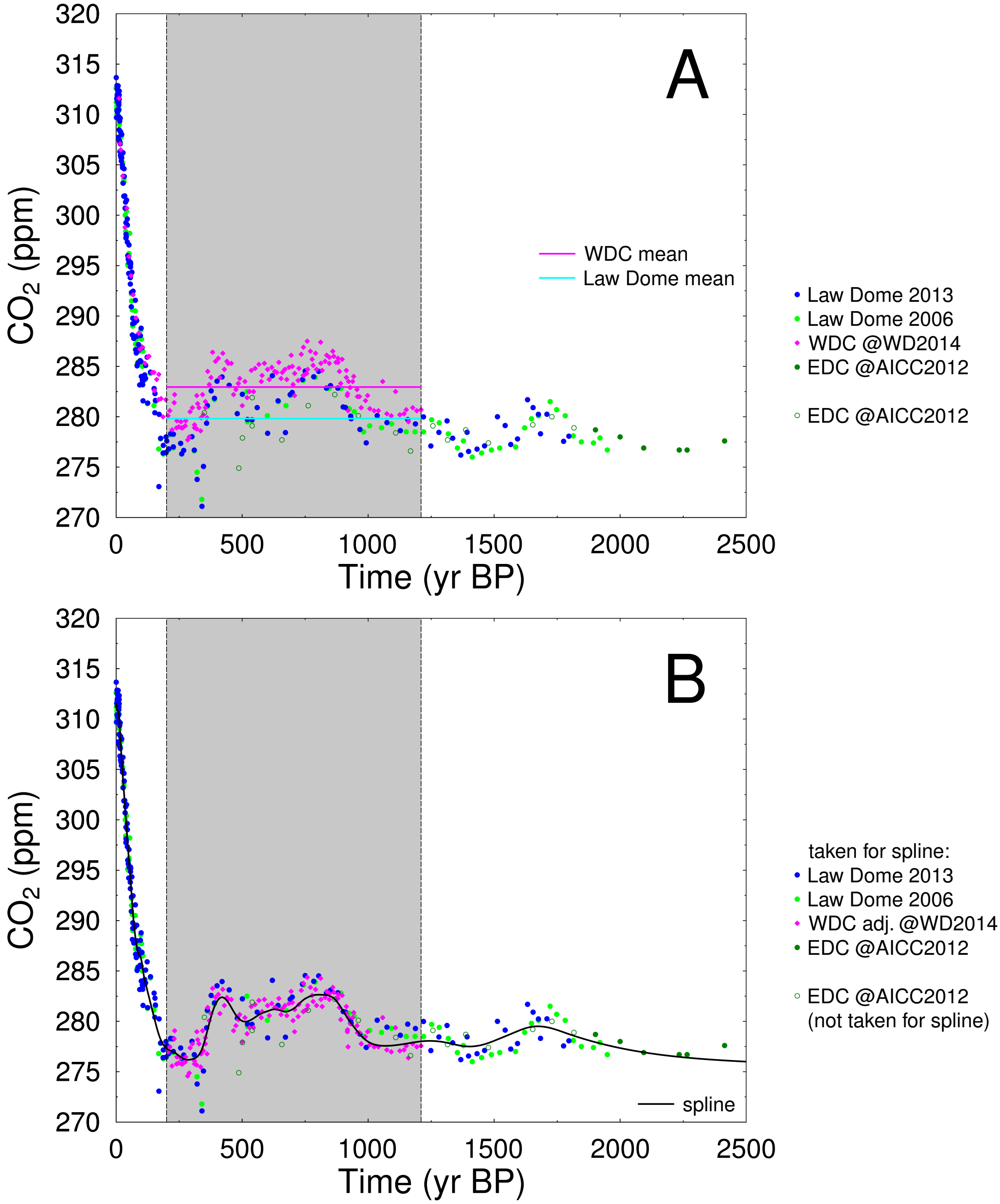

Figure A1: Details of differences between CO_2 of Law Dome (MacFarling-Meure et al., 2006; Rubino et al., 2013), EDC (Monnin et al., 2004) and WDC (Ahn et al., 2012; Bauska et al., 2015) during the last 2000 years and how the adjustment of the WDC has been calculated. Grey area marks the pre-anthropogenic time window (before 1750 CE) covered in WDC (200–1210 BP) from which the difference in CO_2 from WDC and Law Dome records has been determined. Horizontal lines mark the mean values for the different ice cores (cyan: Law Dome (all data); magenta: WDC). The mean offset between the WDC and Law Dome of 3.13 ppm is subtracted from the WDC data in subpanel B.

Earth Syst. Sci. Data Discuss., doi:10.5194/essd-2017-6, 2017
Manuscript under review for journal Earth Syst. Sci. Data
Discussion started: 20 February 2017

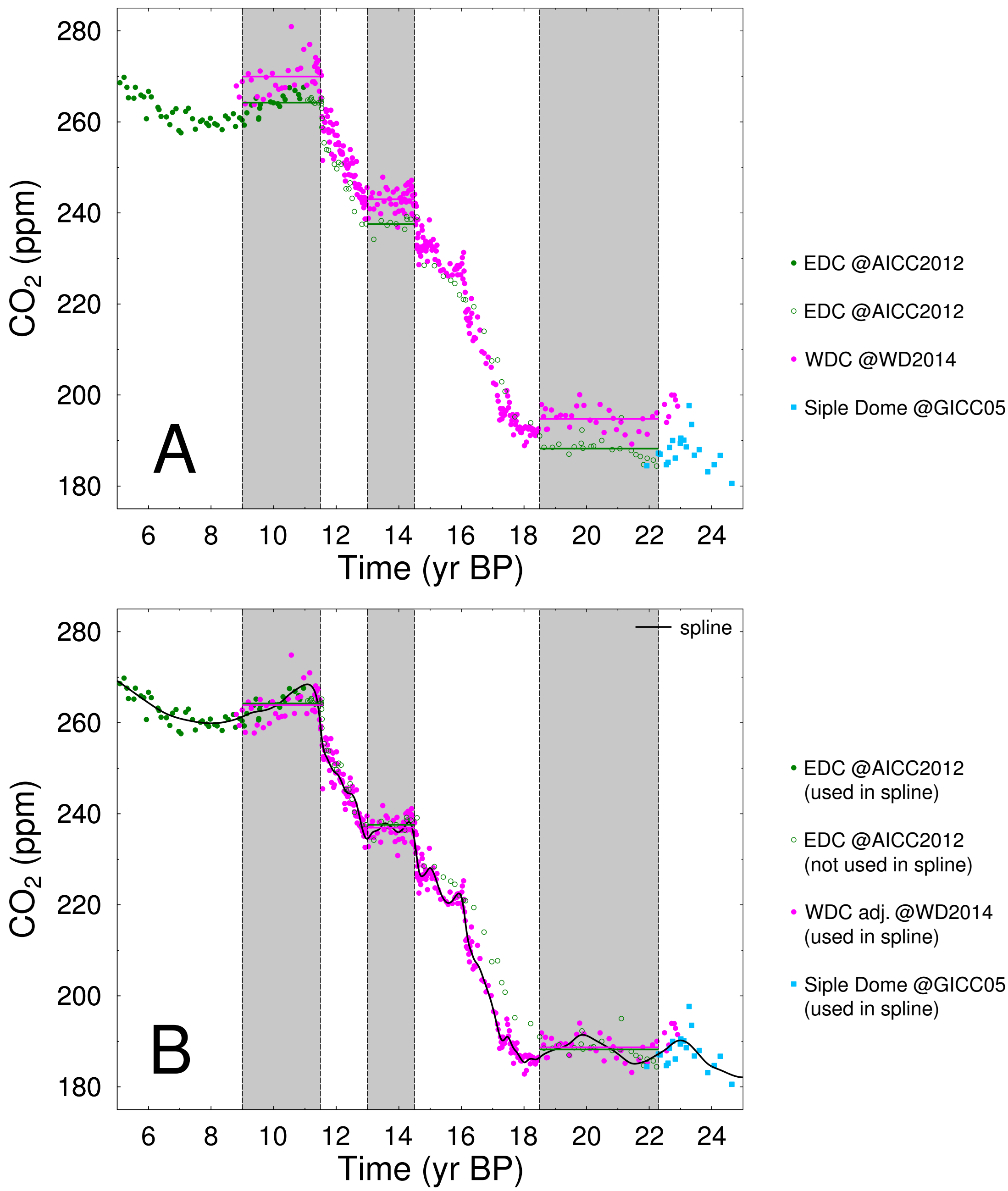

Figure A2: Details of differences between CO_2 of EDC (Monnin et al., 2001, 2004) and WDC (Marcott et al., 2014) during Termination I and how the adjustment of the WDC has been calculated. Grey areas mark the three time windows with relatively stable CO_2 from which the difference in CO_2 from both records has been determined. Horizontal lines mark the mean values for the different ice cores (green: EDC; magenta: WDC). The duration-weighted mean offset between the WDC and EDC of 6.06 ppm is subtracted from the WDC data in subpanel B.